

# Anti-PfGARP activates programmed cell death of parasites and reduces severe malaria

<https://doi.org/10.1038/s41586-020-2220-1>

Received: 22 February 2019

Accepted: 20 February 2020

Published online: 22 April 2020

 Check for updates

Dipak K. Raj<sup>1,2</sup>, Alok Das Mohapatra<sup>1,2</sup>, Anup Jnawali<sup>1,2</sup>, Jenna Zuromski<sup>1,2</sup>, Ambrish Jha<sup>1</sup>, Gerald Cham-Kpu<sup>1,2</sup>, Brett Sherman<sup>1</sup>, Rachel M. Rudlaff<sup>3,4</sup>, Christina E. Nixon<sup>1,2</sup>, Nicholas Hilton<sup>1,19</sup>, Andrew V. Oleinikov<sup>5</sup>, Olga Chesnokov<sup>5</sup>, Jordan Merritt<sup>5</sup>, Sunthorn Pond-Tor<sup>1,2</sup>, Lauren Burns<sup>1,2</sup>, Grant Jolly<sup>2</sup>, Choukri Ben Mamoun<sup>6,7</sup>, Edward Kabyemela<sup>8,9,10</sup>, Atis Muehlenbachs<sup>11</sup>, Lynn Lambert<sup>12</sup>, Sachy Orr-Gonzalez<sup>12</sup>, Nina F. Gnädig<sup>13</sup>, David A. Fidock<sup>13,14</sup>, Sangshin Park<sup>1,15</sup>, Jeffrey D. Dvorin<sup>3,4</sup>, Norbert Pardi<sup>16</sup>, Drew Weissman<sup>16</sup>, Barbara L. Mui<sup>17</sup>, Ying K. Tam<sup>17</sup>, Jennifer F. Friedman<sup>1,18</sup>, Michal Fried<sup>12,20</sup>, Patrick E. Duffy<sup>12,20</sup> & Jonathan D. Kurtis<sup>1,2,20</sup>✉

Malaria caused by *Plasmodium falciparum* remains the leading single-agent cause of mortality in children<sup>1</sup>, yet the promise of an effective vaccine has not been fulfilled. Here, using our previously described differential screening method to analyse the proteome of blood-stage *P. falciparum* parasites<sup>2</sup>, we identify *P. falciparum* glutamic-acid-rich protein (PfGARP) as a parasite antigen that is recognized by antibodies in the plasma of children who are relatively resistant—but not those who are susceptible—to malaria caused by *P. falciparum*. PfGARP is a parasite antigen of 80 kDa that is expressed on the exofacial surface of erythrocytes infected by early-to-late-trophozoite-stage parasites. We demonstrate that antibodies against PfGARP kill trophozoite-infected erythrocytes in culture by inducing programmed cell death in the parasites, and that vaccinating non-human primates with PfGARP partially protects against a challenge with *P. falciparum*. Furthermore, our longitudinal cohort studies showed that, compared to individuals who had naturally occurring anti-PfGARP antibodies, Tanzanian children without anti-PfGARP antibodies had a 2.5-fold-higher risk of severe malaria and Kenyan adolescents and adults without these antibodies had a twofold-higher parasite density. By killing trophozoite-infected erythrocytes, PfGARP could synergize with other vaccines that target parasite invasion of hepatocytes or the invasion of and egress from erythrocytes.

To identify novel vaccine candidates for malaria caused by *P. falciparum*, we pooled plasma collected at two years of age from the most-resistant individuals and the most-susceptible individuals who participated in our Tanzanian birth cohort<sup>3</sup> (Supplementary Table 1) and performed differential biopanning experiments on a *P. falciparum* 3D7 strain blood-stage cDNA library constructed in bacteriophage (hereafter phage) T7. After differentially biopanning  $1.0 \times 10^8$  recombinant phages and sequencing  $n = 100$  differentially recognized clones, we identified 11 parasite genes the protein products of which were uniquely recognized by antibodies in plasma from resistant—but not susceptible—individuals (Supplementary Table 2).

On the basis of its *in silico* properties, its high degree of enrichment (44 out of 100 differentially biopanned clones) and its representation by

clones derived from three overlapping but distinct cDNAs, we focused our attention on PfGARP (encoded by PF3D7\_0113000).

An *in silico* analysis using PlasmoDB<sup>4</sup> ([www.plasmodb.org](http://www.plasmodb.org)) and OrthoMCL-DB<sup>5</sup> ([www.orthomcl.org](http://www.orthomcl.org)) predicted that PF3D7\_0113000 contains a 2,236-bp gene (*PfGARP*) that encodes an 80-kDa acidic protein with a functional *Plasmodium* export element (PEXEL) motif (Supplementary Information, Extended Data Fig. 10), and that has one intron near its 5' end. *PfGARP* has syntenic orthologues in *Plasmodium praefalciparum*, *Plasmodium gaboni* and *Plasmodium reichenowi*, but no orthologues in any other species of *Plasmodium* or in any other organism that has been examined so far. PfGARP has no homology with proteins of known function and contains several complex repeat

<sup>1</sup>Center for International Health Research, Rhode Island Hospital, Brown University Medical School, Providence, RI, USA. <sup>2</sup>Department of Pathology and Laboratory Medicine, Brown University Medical School, Providence, RI, USA. <sup>3</sup>Division of Infectious Diseases, Boston Children's Hospital, Boston, MA, USA. <sup>4</sup>Department of Pediatrics, Harvard Medical School, Boston, MA, USA.

<sup>5</sup>Charles E. Schmidt College of Medicine, Florida Atlantic University, Boca Raton, FL, USA. <sup>6</sup>Department of Internal Medicine, Yale University, New Haven, CT, USA. <sup>7</sup>Department of Microbial Pathogenesis, Yale University, New Haven, CT, USA. <sup>8</sup>Mother Offspring Malaria Studies (MOMS) Project, Seattle Biomedical Research Institute, Seattle, WA, USA. <sup>9</sup>Muheza Designated District Hospital, Muheza, Tanzania. <sup>10</sup>Muhimbili University of Health and Allied Sciences, Dar es Salaam, Tanzania. <sup>11</sup>Infectious Disease Pathology Branch, Centers for Disease Control and Prevention, Atlanta, GA, USA. <sup>12</sup>Laboratory of Malaria Immunology and Vaccinology, National Institute of Allergy and Infectious Diseases, National Institutes of Health, Rockville, MD, USA. <sup>13</sup>Department of Microbiology and Immunology, Columbia University Irving Medical Center, New York, NY, USA. <sup>14</sup>Division of Infectious Diseases, Department of Medicine, Columbia University Irving Medical Center, New York, NY, USA. <sup>15</sup>Graduate School of Urban Public Health, University of Seoul, Seoul, South Korea. <sup>16</sup>Department of Medicine, University of Pennsylvania, Philadelphia, PA, USA. <sup>17</sup>Acuitas Therapeutics, Vancouver, British Columbia, Canada. <sup>18</sup>Department of Pediatrics, Rhode Island Hospital, Brown University Medical School, Providence, RI, USA. <sup>19</sup>Present address: Department of Microbiology and Molecular Genetics, University of California, Davis, Davis, CA, USA. <sup>20</sup>These authors contributed equally: Michal Fried, Patrick E. Duffy, Jonathan D. Kurtis.

✉e-mail: Jonathan\_Kurtis@Brown.edu

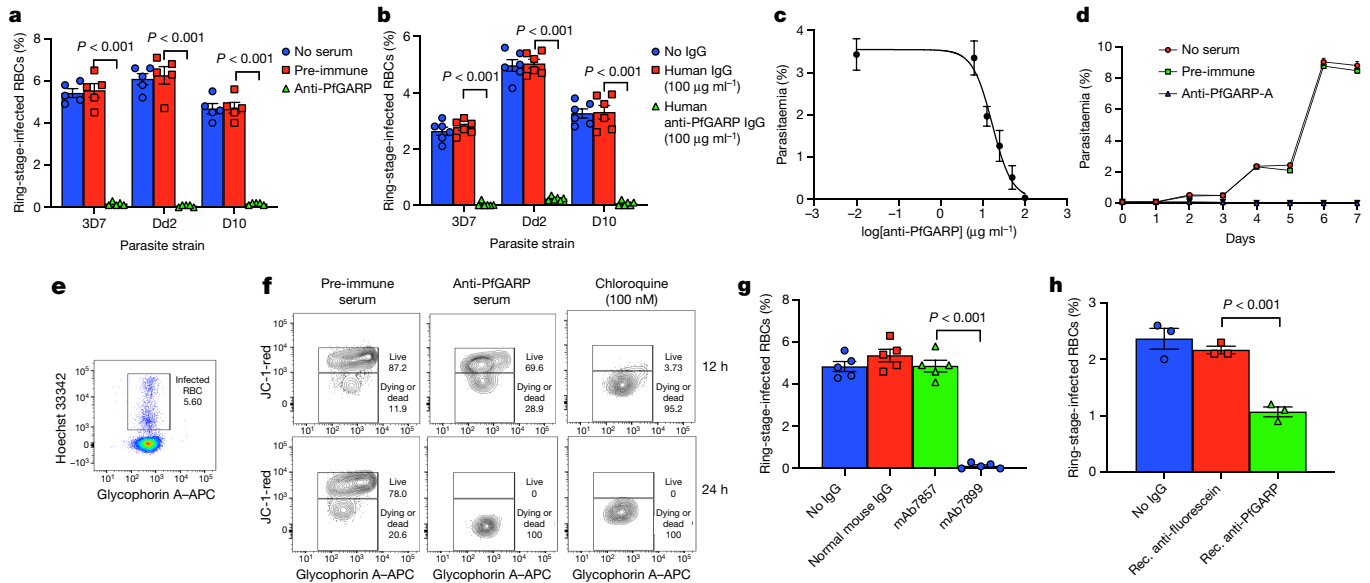


**Fig. 1 | Antibodies to PfGARP inhibit parasite growth.** **a, b,** Mouse anti-PfGARP (1:10 dilution) (green; **a**) or human anti-rPfGARP IgG ( $100 \mu\text{g ml}^{-1}$ ) purified from pooled serum collected from individuals who had been exposed to malaria (green; **b**) inhibits the growth of three different strains of *P. falciparum* (3D7, Dd2 and D10) by 94–99%. Negative controls were no serum (blue) and pre-immune mouse serum (red) (**a**); or control medium with no IgG (blue) and human IgG purified from human serum obtained from malaria-naïve individuals (red) (**b**). Data are mean  $\pm$  s.e.m. of five biologically independent replicates. **c,** The  $\text{IC}_{50}$  of anti-PfGARP purified from sera from vaccinated mice is approximately  $16.8 \mu\text{g ml}^{-1}$ . Data are mean  $\pm$  s.d. of three biologically independent replicates. **d,** Anti-PfGARP kills *P. falciparum* parasites in long-term cultures. Data are mean  $\pm$  s.e.m. of three biologically independent replicates. **e, f,** Anti-PfGARP disrupts mitochondrial membrane potential. RBCs infected with ring-stage 3D7 *P. falciparum* were incubated with pre-immune or anti-PfGARP serum (1:10 dilution) or with chloroquine

(100 nM). **e,** Gating strategy for **f, f,** Contour plots showing infected RBCs with live parasites in the upper gate and dying or dead parasites in the lower gate (defined by JC-1 staining). Data are representative of three independent experiments. **g, h,** Monoclonal anti-PfGARP inhibits parasite growth. **g,** RBCs infected with ring-stage 3D7 *P. falciparum* were cultured with medium alone, normal mouse IgG ( $1 \text{ mg ml}^{-1}$ ) or anti-PfGARP monoclonal antibodies (mAb7857 or mAb7899;  $1 \text{ mg ml}^{-1}$ ). **h,** Recombinant monoclonal anti-PfGARP produced from the sequences of the heavy- and light-chain variable regions of mAb7899 inhibits parasite growth. RBCs infected with ring-stage 3D7 *P. falciparum* were cultured with medium alone, recombinant (rec.) anti-fluorescein ( $250 \mu\text{g ml}^{-1}$ ) or recombinant anti-PfGARP monoclonal antibody ( $250 \mu\text{g ml}^{-1}$ ). Data are mean  $\pm$  s.e.m. of three biologically independent replicates. All *P* values were calculated by two-sided non-parametric Mann–Whitney *U*-test. Data in **a** are representative of five independent experiments. Data in **b–h** are representative of three independent experiments.

regions and extensive regions of low amino-acid complexity; 50% of the protein is composed of three amino acids (Lys, Glu and Asp).

Expression of *PfGARP* is highly restricted to the early-trophozoite stage of the parasite life cycle<sup>6</sup> and the gene shows minimal sequence variation in the immunorelevant region—the region encoded by the largest clone identified in resistant sera from our differential screens (nucleotides 1,222–2,022). A previous deep-sequencing analysis of 227 field samples identified only one non-synonymous single-nucleotide polymorphism (SNP) in the immunorelevant region<sup>7</sup>, and an expanded (as yet unpublished) analysis of 3,248 field samples has provisionally identified 15 non-synonymous SNPs in this region ([https://www.malariagen.net/apps/pf/4.0/#doc=Doc\\*AboutData.htm](https://www.malariagen.net/apps/pf/4.0/#doc=Doc*AboutData.htm)).

### Anti-PfGARP-A kills parasites in vitro

We expressed and purified the polypeptide encoded by the differentially recognized, immunorelevant region of PfGARP from the referent *P. falciparum* 3D7 strain (nucleotides 1,228–2,022; amino acids 410–673) in *Escherichia coli* and designated this recombinant protein rPfGARP-A (Extended Data Fig. 1a). In addition, we cloned this immunorelevant region into a eukaryotic expression plasmid (VR2001). To generate anti-PfGARP-A antiserum, we immunized mice either with the recombinant protein (rPfGARP-A) in TiterMax adjuvant, or with the eukaryotic expression plasmid. In a western blot analysis, both the anti-PfGARP-A antiserum that was generated by immunization with the recombinant protein and the antiserum generated by immunization with DNA recognized a protein of around 100 kDa in trophozoite-infected red blood cells (RBCs) (Extended Data Fig. 1b, k). This higher apparent molecular weight is consistent with the acidic composition of PfGARP<sup>8</sup>.

We performed growth-inhibition assays (GIAs) using anti-PfGARP-A antiserum that was prepared by immunizing mice with either DNA or recombinant protein. Anti-PfGARP-A inhibited parasite growth by 94–99% compared to controls in three parasite strains and four freshly isolated parasite lines (all  $P < 0.001$ ; Fig. 1a, Extended Data Fig. 1d). Anti-PfGARP-A-treated parasites displayed a dysmorphic, pyknotic appearance on Giemsa-stained blood smears, consistent with ‘crisis’ forms that are associated with dying or dead parasites<sup>9,10</sup> (Extended Data Fig. 1e–h).

We purified human polyclonal anti-PfGARP-A antibodies from plasma pooled from adults living in our Tanzanian field site (Extended Data Fig. 1i, j), and found that these human anti-PfGARP-A antibodies significantly inhibited parasite growth by 94–99% compared with controls in three parasite strains (all  $P < 0.001$ , Fig. 1b). In addition, we purified mouse polyclonal anti-PfGARP-A antibodies from plasma pooled from rPfGARP-A-immunized mice (Extended Data Fig. 1k, l), and calculated that the half-maximum inhibitory concentration ( $\text{IC}_{50}$ ) for parasite growth was  $16.8 \mu\text{g}$  of anti-PfGARP-A per ml of culture medium (Fig. 1c).

In long-term cultures, anti-PfGARP-treated parasites never expanded in number (Fig. 1d), and by day two they had decreased in size and appeared pyknotic. By day four, the parasites had become small, pyknotic dots that were difficult to visualize, and by day six, they were no longer identifiable as parasite-infected RBCs. These data indicate that anti-PfGARP antibodies kill parasite-infected RBCs even in the absence of complement or cellular effector functions.

We performed GIA assays and quantified the viability of parasites by flow cytometry using JC-1, a mitochondrial membrane potential probe. Ring-stage parasites that were treated with anti-PfGARP antibodies showed a marked loss of mitochondrial membrane potential

# Article

(a characteristic of programmed cell death) within 12 h, and almost all parasites had lost their mitochondrial function within 24 h (Fig. 1e, f).

We produced a series of monoclonal antibodies in mice that were immunized with rPfGARP-A. Of the sixteen monoclonal antibodies that reacted with PfGARP-A in an enzyme-linked immunosorbent assay (ELISA), only mAb7899 killed parasites in culture (Fig. 1g). We sequenced and expressed the heavy-chain and light-chain variable regions of mAb7899. The resulting recombinant monoclonal antibody had a dissociation constant ( $K_d$ ) of 2.9 nM (95% confidence interval (CI) [1.3, 5.9]; Extended Data Fig. 2a), inhibited parasite growth by 51% at a concentration of 250  $\mu\text{g ml}^{-1}$  in GIA assays (Fig. 1h) and recognized amino acids 443–459 (VKNVIEDKDGVEIIN) of full-length PfGARP (Extended Data Fig. 2b). Consistent with the loss of mitochondrial function, the levels of lactate in the medium of cultures treated with recombinant mAb7899 were significantly higher than those in control cultures (Extended Data Fig. 2c). A monovalent antigen-binding fragment (Fab) of mAb7899 inhibited parasite growth by 76–87% across three strains of *P. falciparum* (Extended Data Fig. 2d). These data confirm that anti-PfGARP-mediated killing occurs in the absence of complement, cellular effector functions or antigen cross-linking.

We used the TetR system<sup>11</sup> to construct parasites with a conditional knockdown of PfGARP (3D7-PfGARP KD) (Extended Data Fig. 3a, Supplementary Table 3). The 3D7-PfGARP KD parasites, when grown in the absence of the inducer anhydrotetracycline, did not exhibit an overt growth phenotype in vitro, despite showing a reduction of up to 90% in the levels of PfGARP protein (Extended Data Fig. 3b–e). In GIA assays, the killing efficacy of anti-PfGARP antibodies was only mildly reduced in 3D7-PfGARP KD parasites cultured without anhydrotetracycline compared to those cultured with it ( $P = 0.014$ ; Extended Data Fig. 3f). Anti-PfGARP-mediated killing of 3D7-PfGARP KD parasites cultured without anhydrotetracycline may be due to the residual expression of PfGARP even in the absence of the inducer. To test this hypothesis, we constructed parasites in which the *PfGARP* gene was deleted (3D7-PfGARP KO) (Extended Data Fig. 4a–d), and evaluated them in growth and GIA assays. The 3D7-PfGARP KO parasites did not exhibit an overt growth phenotype in vitro (Extended Data Fig. 4e). As expected, the killing efficacy of anti-PfGARP antibodies was completely abrogated in the 3D7-PfGARP KO compared to the wild-type parasites (Extended Data Fig. 4f).

## Immunolocalization of PfGARP

To assess the immunolocalization of PfGARP, we used immunofluorescence confocal microscopy and immunogold transmission electron microscopy in 3D7 *P. falciparum* parasites probed with anti-PfGARP. We also evaluated 3D7-PfGARP KD parasites, in which PfGARP is linked to a C-terminal V5 tag, probed with anti-V5 antibodies. In all experiments, PfGARP was localized to the exofacial surface of the RBC membrane in early-to-late-trophozoite-infected RBCs (Extended Data Figs. 5–7).

## Anti-PfGARP disrupts food vacuole integrity

In transmission electron microscopy studies, the food vacuole in anti-PfGARP treated parasites was markedly diminished in size compared to control-treated parasites and appeared absent or condensed tightly around hemozoin crystals—an effect that has not been reported for any previous antimalarial antibodies (Extended Data Fig. 8a, b). We explored the possibility that PfGARP also localized to the membrane of the food vacuole by colocalization studies with the *P. falciparum* chloroquine resistance transporter (PfCRT). In the majority of infected RBCs, PfCRT and PfGARP did not colocalize (Extended Data Fig. 7d). We assessed the effect of anti-PfGARP by confocal microscopy using the calcium-binding dye Fluo-4 AM, which preferentially labels the food vacuole<sup>12</sup>. Parasites treated with anti-PfGARP showed a marked loss of integrity of the food vacuole, as evidenced by the redistribution of Fluo-4 AM (and therefore calcium) from the food vacuole<sup>12</sup> to the cytosol (Extended Data Fig. 8c). We further evaluated the effect of anti-PfGARP antibodies on

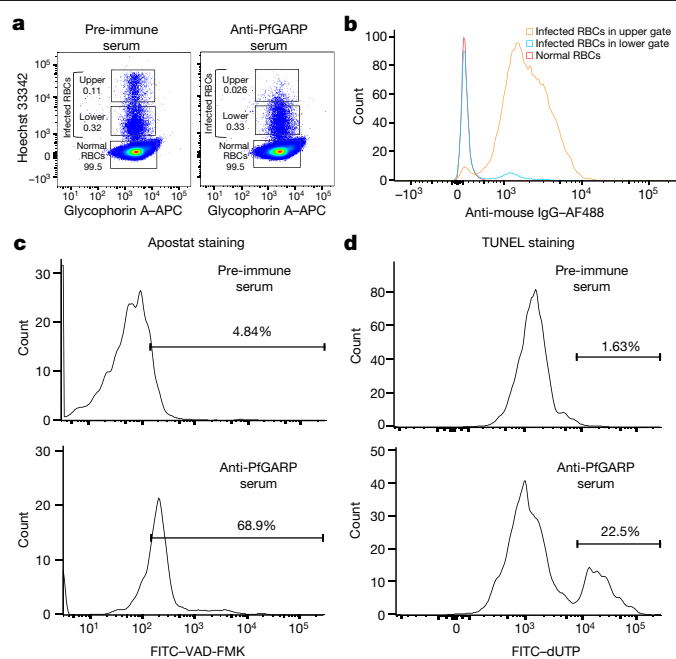


**Fig. 2 | Antibodies to PfGARP bind to *P. falciparum*-infected RBCs, leading to the activation of caspase-like proteases and the fragmentation of parasite DNA.** **a**, RBCs infected with ring-stage 3D7 *P. falciparum* were cultured for 24–30 h in the presence of 10% mouse pre-immune or anti-PfGARP serum that was generated by vaccination with DNA. Representative dot plots show infected RBCs with a higher DNA content (mature parasites) in the upper gate, infected RBCs with a lower DNA content (immature and dying parasites) in the middle gate and uninfected RBCs in the lowest gate. **b**, Binding of polyclonal anti-PfGARP antibodies to the infected RBCs in the upper two gates and the uninfected RBCs in the lowest gate from **a**. **c, d**, Incubation of infected RBCs with anti-PfGARP results in the activation of caspase-like proteases (assessed by Apostat staining; **c**) and DNA fragmentation (assessed by TUNEL staining; **d**) in parasites that were present in the upper gate. Percentages in **c, d** indicate the proportion of gated events occurring within the range bounded by the horizontal line. All data are representative of three independent experiments.

food vacuole integrity using serial block-face scanning electron microscopy (SBF-SEM), which demonstrated that treatment with anti-PfGARP resulted in a complete loss of food vacuole integrity, with hemozoin dispersed broadly throughout the parasitophorous vacuole (Supplementary Video 1).

## Anti-PfGARP activates programmed cell death

The effect of anti-PfGARP antibodies on parasite morphology, mitochondrial membrane potential and food vacuole integrity (with increased intracellular levels of calcium) suggests parasites are killed through the activation of programmed cell death. We therefore analysed anti-PfGARP-treated parasites for the activation of caspase-like enzymes. We performed GIA assays and probed the parasites with Apostat, a fluorescent dye that labels activated-caspase-like cysteine proteases. Parasites that were treated with anti-PfGARP showed a marked increase in the activation of caspase-like proteases compared to untreated parasites, as assessed by flow cytometry (Fig. 2a–c). We also performed TUNEL (terminal deoxynucleotidyl transferase dUTP nick-end labelling) assays to determine whether treatment with anti-PfGARP resulted in the fragmentation of parasite DNA. Parasites that were treated with anti-PfGARP showed substantial fragmentation of their DNA, as assessed by flow cytometry (Fig. 2d).

## Tanzanian birth cohort study

To investigate the effects of naturally acquired anti-PfGARP antibodies on clinical malaria, we measured the levels of anti-PfGARP IgG antibodies in

members of our Tanzanian birth cohort using a fluorescent, bead-based assay, and related the results to subsequent malaria outcomes.

We measured the levels of anti-PfGARP IgG antibodies in plasma that was obtained from 246 children at the age of 48 weeks. The average duration of follow-up was 64 weeks per child. Anti-PfGARP antibodies were detectable in 48.8% of these samples and children were followed for a total of 15,737 child weeks of observation.

We used generalized estimating equation (GEE)-based repeated measures models to evaluate the relationship between the levels of anti-PfGARP IgG and the risk of severe malaria. When analysed as a continuous variable, anti-PfGARP IgG levels predicted a significantly decreased risk of severe malaria over the follow-up period ( $P = 0.008$ ). When analysed dichotomously, individuals with undetectable anti-PfGARP IgG antibodies ( $n = 126$  individuals who contributed 7,327 weeks of follow-up) had a 2.5-fold-higher risk of severe malaria than individuals with detectable anti-PfGARP IgG antibodies ( $n = 120$  individuals who contributed 8,410 weeks of follow-up; 95% CI [1.2, 5.5],  $P = 0.018$ ) (Fig. 3a). These results remained significant (odds ratio = 2.5, 95% CI [1.1, 5.5],  $P = 0.026$ ) even after adjusting for potential confounders (see Supplementary Methods for the modelling approach).

### Kenyan cohort study

To generalize these results to a completely independent cohort, we measured anti-rPfGARP-A IgG responses in a cohort of Kenyan male individuals who participated in a treatment-reinfection study<sup>13–15</sup>. Volunteers ( $n = 135$ ) aged 12–35 years were entered into the study at the beginning of the high-transmission season in April 1997, treated for malaria and followed with weekly blood smears for 18 weeks. Serum was collected two weeks after treatment and stored at  $-80^{\circ}\text{C}$ . In this age group, clinical or severe malaria is very uncommon.

When analysed as a continuous variable in GEE-based repeated measures models, higher anti-PfGARP IgG levels predicted a significantly decreased parasite density over 18 weeks of follow-up ( $P < 0.004$ ). When analysed dichotomously, individuals with undetectable anti-rPfGARP-A IgG antibodies ( $n = 61$  individuals who contributed 1,018 weeks of follow-up blood smears) had 1.97-fold higher densities of parasites over the 18 weeks of follow-up than individuals who had detectable anti-rPfGARP-A IgG antibodies ( $n = 74$  individuals who contributed 1,237 weeks of follow-up blood smears; 95% CI [0.94, 4.23],  $P = 0.012$ ) (Fig. 3b). These results remained significant (odds ratio = 1.82, 95% CI [0.9, 3.7],  $P = 0.019$ ) after adjusting for potential confounders (see Supplementary Methods).

### Monkey vaccine trials

Because PfGARP is only found in *Plasmodium* species that infect primates, we conducted a vaccine trial in the *P. falciparum*/*Aotus* model, in which *Aotus* monkeys are infected with *P. falciparum*. Nucleoside-modified mRNA vaccines (purified by fast protein liquid chromatography (FPLC)) against the Zika and influenza viruses have been shown to have potent effects in small and large animals<sup>16–18</sup>. We therefore immunized  $n = 5$  monkeys intradermally with 50  $\mu\text{g}$  of nucleoside-modified mRNA encoding PfGARP-A, encapsulated in lipid nanoparticles (PfGARP-A-mRNA LNPs). Control monkeys ( $n = 4$ ) were intradermally immunized with 50  $\mu\text{g}$  of LNPs containing poly(C) RNA (poly(C)-RNA LNPs). The monkeys received three doses at three-week intervals, and before each dose, serum was obtained for antibody assays. On day 63, the monkeys were challenged by intravenous injection with  $1 \times 10^4$  RBCs infected with blood-stage *P. falciparum* FVO strain parasites, and blood films were prepared daily. This represents a heterologous challenge with a highly virulent parasite as the sequence for the PfGARP-A-mRNA LNP vaccine was derived from the 3D7 strain.

Immunized monkeys generated antibody responses that plateaued after the second injection (Fig. 4a). Control monkeys had significantly

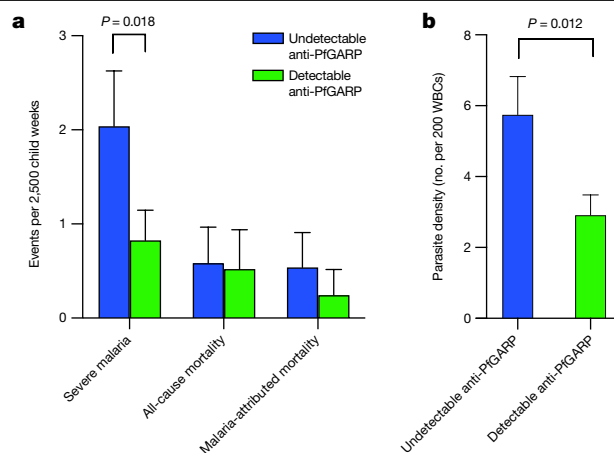


**Fig. 3 | Antibodies to PfGARP predict a reduced risk of severe malaria and parasitaemia. a**, Tanzanian children with undetectable anti-PfGARP IgG antibodies at the age of 48 weeks ( $n = 126$  individuals who contributed 7,327 weeks of follow-up) had a 2.5-fold-higher risk of developing severe malaria than children who had detectable anti-PfGARP IgG antibodies at this age ( $n = 120$  individuals who contributed 8,410 weeks of follow-up; 95% CI [1.2, 5.5],  $P = 0.018$ , GEE model with two-sided fixed-effect test). Bars represent the least-square mean number of events per 2,500 child weeks, with s.e.m. adjusted for repeated measures. **b**, Kenyan male individuals with undetectable anti-rPfGARP-A IgG antibodies ( $n = 61$  individuals who contributed 1,018 weeks of follow-up blood smears) had 1.97-fold-higher parasite densities over 18 weeks of follow-up than did individuals with detectable IgG anti-rPfGARP-A antibodies ( $n = 74$  individuals who contributed 1,237 weeks of follow-up blood smears; 95% CI [0.94, 4.23],  $P = 0.012$ , GEE model with two-sided fixed-effect test). Bars depict the least-square mean parasite density (measured as the number of asexual-stage parasites per 200 white blood cells (WBCs)) with s.e.m.

higher parasitaemia on day 12 than monkeys that were immunized with PfGARP-A ( $P < 0.009$ ), with 4.6-fold-higher parasitaemia on day 13, the final day with complete follow-up of all monkeys ( $P < 0.001$ , Fig. 4b). On day 13, all of the control monkeys met pre-specified criteria for antimalarial treatment (parasitaemia  $> 7.5\%$ ). Of the five PfGARP-A-vaccinated monkeys, one was treated for hyperparasitaemia on day 16 and one for hyperparasitaemia on day 17; one was treated for anaemia—a common complication in the *Aotus/P. falciparum* model<sup>19</sup>—on day 17; and the two remaining monkeys were treated for anaemia on day 18, despite controlling their parasitaemia (Extended Data Fig. 9a). Notably, the three monkeys that controlled their parasitaemia and required treatment for anaemia had higher anti-PfGARP titres (16,000, 16,000 and 32,000) compared to the monkeys that required treatment for their parasitaemia (8,000 and 4,000).

We also conducted a trial in the *P. falciparum*/*Aotus* model using rPfGARP-A (expressed in *E. coli*) emulsified in Ribi adjuvant as the immunogen. We immunized monkeys subcutaneously with 50  $\mu\text{g}$  of either PfGARP-A in Ribi adjuvant ( $n = 4$  monkeys) or Ribi alone ( $n = 5$  monkeys). The monkeys received three doses at three-week intervals, and before each dose, samples of serum were obtained for antibody assays. On day 63, the monkeys were challenged by intravenous injection with  $1 \times 10^4$  RBCs infected with blood-stage *P. falciparum* FVO strain parasites, and blood films were produced daily. Immunized monkeys generated antibody responses that increased after the third injection (Extended Data Fig. 9b). Notably, control monkeys had significantly higher parasitaemia on days 7–12 than PfGARP-A-vaccinated monkeys (all  $P < 0.05$ ; Extended Data Fig. 9c, d). On day 11—the final day with complete follow-up of all monkeys—control monkeys had 3.5-fold-higher parasitaemia than PfGARP-A-vaccinated monkeys ( $P < 0.01$ ). Four control monkeys met pre-specified criteria for drug treatment (parasitaemia greater than 7.5%, haematocrit lower than 25% or evidence of clinical illness) on day 11, and the remaining control monkey met these criteria

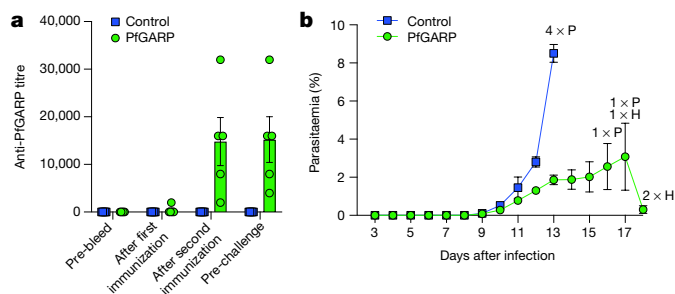


**Fig. 4 | Vaccination with PfGARP-A-mRNA LNPs protects monkeys from challenge with *P. falciparum*.** **a**, *Aotus* monkeys were intradermally injected with 50 µg of PfGARP-A-mRNA LNPs ( $n = 5$  monkeys) or 50 µg of poly(C)-RNA LNPs (negative control;  $n = 4$  monkeys) at weeks 0, 3 and 6, and PfGARP-specific IgG titres were determined. Data are mean  $\pm$  s.e.m. **b**, Vaccinated *Aotus* monkeys were challenged intravenously with  $1 \times 10^4$  blood-stage *P. falciparum* FVO strain-infected RBCs on day 63 and parasitaemia was followed daily. Data are mean  $\pm$  s.e.m. Control monkeys had significantly higher parasitaemia on day 12 than monkeys immunized with PfGARP-A ( $P < 0.009$ , two-sided  $t$ -test), with 4.6-fold-higher parasitaemia on day 13, the final day with complete follow-up of all monkeys ( $P < 0.001$ , two-sided  $t$ -test). On day 13, all control monkeys required antimalarial treatment for high parasitaemia (indicated by 4 × P). On day 16, one vaccinated monkey required treatment for high parasitaemia (1 × P). On day 17, one vaccinated monkey required treatment for high parasitaemia and one required treatment for low haemoglobin (1 × H). On day 18, two vaccinated monkeys required treatment for low haemoglobin (2 × H).

on day 12. On day 11, one PfGARP-vaccinated monkey underwent drug treatment despite not meeting the pre-specified criteria.

### Summary and conclusions

Malaria remains a leading cause of childhood mortality and vaccines are urgently needed to attenuate this threat to public health. Using our vaccine discovery platform, we identified PfGARP—an antigen that is localized to the exofacial surface of the RBC membrane in trophozoite-infected RBCs—as a vaccine candidate targeting the blood stage of *P. falciparum*. Anti-PfGARP markedly attenuates the growth of parasites by arresting and killing trophozoite-infected RBCs in the absence of immune effector cells or complement.

Parasites that were treated with anti-PfGARP displayed several canonical features of programmed cell death, including shrunken, pyknotic nuclei; a loss of mitochondrial membrane integrity; the activation of caspase-like proteases; DNA fragmentation; and the release of calcium from intracellular stores. Although *P. falciparum* lacks classic caspases, it does encode three meta-caspases<sup>20</sup>, and activation of *P. falciparum* metacaspase 1 (PfMCA1) functions as an upstream activator of a caspase-like enzyme that leads to programmed cell death<sup>21</sup>. This ability to induce programmed cell death in *Plasmodium* parasites is a novel mode of action for an antimalarial antibody. Because PfGARP is located on the exofacial surface of RBCs, and because antibody engagement of PfGARP leads to the activation of programmed cell death in parasites, we speculate that PfGARP might function in the density-dependent regulation of parasitaemia by sensing either parasite or host factors<sup>22–24</sup>.

In non-human primates, immunization with PfGARP as either an mRNA-based or a recombinant-protein-based immunogen conferred marked protection against parasitaemia compared with controls after a heterologous challenge with *P. falciparum*. This is the first report, to our knowledge, of an mRNA-based vaccine that induces protection against *P. falciparum*.

In longitudinal cohort studies, naturally occurring anti-PfGARP predicted a decreased risk of severe malaria in children and decreased parasitaemia in adolescents and adults. Together, our data support PfGARP as a vaccine candidate against malaria caused by *P. falciparum*.

Furthermore, our recombinant monoclonal anti-PfGARP antibody could serve as a platform for the development of therapeutic and prophylactic antibody-based interventions, and could also be used in high-throughput drug screens that target PfGARP-induced programmed cell death. By killing trophozoite-infected RBCs, immunization with PfGARP could synergize with other vaccines that target the parasite invasion of hepatocytes<sup>25</sup> or the invasion of and egress from erythrocytes<sup>2,26</sup>.

### Online content

Any methods, additional references, Nature Research reporting summaries, source data, extended data, supplementary information, acknowledgements, peer review information; details of author contributions and competing interests; and statements of data and code availability are available at <https://doi.org/10.1038/s41586-020-2220-1>.

- World Health Organization. *World Health Statistics 2018: Monitoring Health for the SDGs* <https://www.who.int/data/gho/publications/world-health-statistics> (WHO, 2018).
- Raj, D. K. et al. Antibodies to PfSEA-1 block parasite egress from RBCs and protect against malaria infection. *Science* **344**, 871–877 (2014).
- Mutabingwa, T. K. et al. Maternal malaria and gravidity interact to modify infant susceptibility to malaria. *PLoS Med.* **2**, e407 (2005).
- Aurrecochea, C. et al. PlasmoDB: a functional genomic database for malaria parasites. *Nucleic Acids Res.* **37**, D539–D543 (2009).
- Chen, F., Mackey, A. J., Stoeckert, C. J. Jr & Roos, D. S. OrthoMCL-DB: querying a comprehensive multi-species collection of ortholog groups. *Nucleic Acids Res.* **34**, D363–D368 (2006).
- López-Barragán, M. J. et al. Directional gene expression and antisense transcripts in sexual and asexual stages of *Plasmodium falciparum*. *BMC Genomics* **12**, 587 (2011).
- Manske, M. et al. Analysis of *Plasmodium falciparum* diversity in natural infections by deep sequencing. *Nature* **487**, 375–379 (2012).
- Tiwari, P., Kaila, P. & Guptasarma, P. Understanding anomalous mobility of proteins on SDS-PAGE with special reference to the highly acidic extracellular domains of human E- and N-cadherins. *Electrophoresis* **40**, 1273–1281 (2019).
- Ockenhouse, C. F., Schulman, S. & Shear, H. L. Induction of crisis forms in the human malaria parasite *Plasmodium falciparum* by gamma-interferon-activated, monocyte-derived macrophages. *J. Immunol.* **133**, 1601–1608 (1984).
- Jensen, J. B., Boland, M. T. & Akood, M. Induction of crisis forms in cultured *Plasmodium falciparum* with human immune serum from Sudan. *Science* **216**, 1230–1233 (1982).
- Ganesan, S. M., Falla, A., Goldfless, S. J., Nasamu, A. S. & Niles, J. C. Synthetic RNA-protein modules integrated with native translation mechanisms to control gene expression in malaria parasites. *Nat. Commun.* **7**, 10727 (2016).
- Ch'Ng, J. H., Liew, K., Goh, A. S., Sidhartha, E. & Tan, K. S. Drug-induced permeabilization of parasite's digestive vacuole is a key trigger of programmed cell death in *Plasmodium falciparum*. *Cell Death Dis.* **2**, e216 (2011).
- Kurtis, J. D., Lanar, D. E., Opollo, M. & Duffy, P. E. Interleukin-10 responses to liver-stage antigen 1 predict human resistance to *Plasmodium falciparum*. *Infect. Immun.* **67**, 3424–3429 (1999).
- Kurtis, J. D., Mtalib, R., Onyango, F. K. & Duffy, P. E. Human resistance to *Plasmodium falciparum* increases during puberty and is predicted by dehydroepiandrosterone sulfate levels. *Infect. Immun.* **69**, 123–128 (2001).
- Nixon, C. P. et al. Antibodies to rhothry-associated membrane antigen predict resistance to *Plasmodium falciparum*. *J. Infect. Dis.* **192**, 861–869 (2005).
- Pardi, N. et al. Nucleoside-modified mRNA vaccines induce potent T follicular helper and germinal center B cell responses. *J. Exp. Med.* **215**, 1571–1588 (2018).
- Pardi, N. et al. Zika virus protection by a single low-dose nucleoside-modified mRNA vaccination. *Nature* **543**, 248–251 (2017).
- Pardi, N. et al. Nucleoside-modified mRNA immunization elicits influenza virus hemagglutinin stalk-specific antibodies. *Nat. Commun.* **9**, 3361 (2018).
- Egan, A. F., Fabucci, M. E., Saul, A., Kaslow, D. C. & Miller, L. H. *Aotus* New World monkeys: model for studying malaria-induced anemia. *Blood* **99**, 3863–3866 (2002).
- Vandana, D., Dixit, R., Tiwari, R., Katyal, A. & Pandey, K. C. Metacaspases: potential drug target against protozoan parasites. *Front. Pharmacol.* **10**, 790 (2019).
- Meslin, B., Beavogui, A. H., Fasel, N. & Picot, S. *Plasmodium falciparum* metacaspase PfMCA-1 triggers a z-VAD-fmk inhibitable protease to promote cell death. *PLoS One* **6**, e23867 (2011).
- Mutai, B. K. & Waitumbi, J. N. Apoptosis stalks *Plasmodium falciparum* maintained in continuous culture condition. *Malar. J.* **9**, S6 (2010).
- Engelbrecht, D. & Coetzer, T. L. *Plasmodium falciparum* exhibits markers of regulated cell death at high population density in vitro. *Parasitol. Int.* **65**, 715–727 (2016).
- Chou, E. S. et al. A high parasite density environment induces transcriptional changes and cell death in *Plasmodium falciparum* blood stages. *FEBS J.* **285**, 848–870 (2018).
- RTS,S Clinical Trials Partnership. First results of phase 3 trial of RTS,S/AS01 malaria vaccine in African children. *N. Engl. J. Med.* **365**, 1863–1875 (2011).
- Crosnier, C. et al. Basigin is a receptor essential for erythrocyte invasion by *Plasmodium falciparum*. *Nature* **480**, 534–537 (2011).

**Publisher's note** Springer Nature remains neutral with regard to jurisdictional claims in published maps and institutional affiliations.

© The Author(s), under exclusive licence to Springer Nature Limited 2020

## Methods

### Data reporting

No statistical methods were used to predetermine sample size. The experiments were not randomized. The investigators were blinded to allocation during the non-human primate experiments and outcome assessments. Investigators were blinded to clinical status during blood-smear reading for the human cohort studies.

### Ethical approval

The study complied with all relevant ethical regulations for both animal and human studies. Ethical clearance was obtained from the institutional review boards of Seattle Biomedical Research Institute and Rhode Island Hospital; the Medical Research Coordinating Committee of the National Institute for Medical Research, Tanzania; and the Kenyan Medical Research Institute. Ethical clearance for animal studies was obtained from the relevant review boards of Brown University, Rhode Island Hospital and the US National Institutes of Health (NIH).

### Tanzanian birth cohort

**Study population.** Volunteers participated in the Mother Offspring Malaria Studies (MOMS) project, which is based at Muheza Designated District Hospital, in northeastern Tanzania. Mothers presenting at Muheza Designated District Hospital for delivery were enrolled and provided signed, informed consent for their participation, and that of their newborns, in the study. The entomological inoculation rate in our study site exceeds 400 infectious mosquito bites per person per year<sup>27</sup>. Details of the MOMS study design, enrolment methods and exclusion criteria have been published elsewhere<sup>3,28</sup>.

**Inclusion criteria and clinical monitoring.** We monitored 785 children for *P. falciparum* infection from birth up to 3.5 years of age. Children were evaluated at routine 'well-child' visits by a clinician every two weeks from birth to one year of age, and monthly thereafter, including analysis of blood smears. Routine blood samples were collected once every 6 months from the age of 1.5 to 3.5 years. Blood smears and blood samples were also collected any time the child became sick. Sick children who came to hospitals or mobile clinics were examined by a medical officer. Treatment outside the study was minimized by active, weekly surveillance by our mobile clinics.

Clinical malaria was defined as asexual *P. falciparum* parasitaemia by blood smear, coupled with symptoms suggestive of malaria, such as a temperature higher than 37.5 °C, nausea or vomiting, irritability and poor feeding. Prompt treatment was provided to sick children according to the guidelines of the Tanzanian Ministry of Health, and study participants were instructed to obtain all medications including antimalarial drugs through the project staff.

**Sample collection and processing.** Venous blood was collected and stored at 4 °C until processing. After centrifugation, plasma was stored at -80 °C. *P. falciparum* parasitaemia was determined by Giemsa staining of thick blood smears prepared from the capillary or venous blood. Parasite density was expressed as the number of asexual-stage parasites per 200 white blood cells in the thick smear. Sickle cell trait was determined by electrophoresis (Helena Laboratories). Haemograms were obtained on an impedance-based analyser (Abbott Cell Dye 1200).

**Case definitions.** Mild malaria was defined as a positive blood smear and one or more of the following: (1) anaemia defined by a blood haemoglobin level of less than 8 g dl<sup>-1</sup>; (2) vomiting; (3) diarrhoeal disease or gastroenteritis; (4) lower respiratory infection; or (5) oral temperature higher than 38 °C.

Severe malaria was defined as a positive blood smear and one or more of the following: (1) respiratory distress defined by respiratory rate exceeding 40 breaths per minute for children older than two months

or 50 breaths per minute for children younger than two months; (2) a history of one or more convulsions in the 24 h before or during hospitalization; (3) prostration defined by inability to sit unaided; (4) hypoglycaemia defined by a blood glucose level of less than 2.2 mmol l<sup>-1</sup>; (5) severe anaemia defined by a blood haemoglobin level of less than 6 g dl<sup>-1</sup>; or (6) oral temperature higher than 40 °C.

Malaria-associated mortality was defined as death with a positive blood film obtained during the terminal illness. One child who died of bacterial meningitis but had a positive blood film was adjudicated as a non-malarial death.

### Kenyan cohort

**Study population.** To generalize the protective nature of anti-PfGARP antibodies, we measured the levels of anti-PfGARP antibody in an entirely distinct longitudinal cohort using epidemiological data and blood samples that were collected in 1997 as part of a treatment-reinfection study<sup>14,29</sup>. Volunteers were residents of subsistence-farming villages in which *P. falciparum* is endemic, in western Kenya north of Lake Victoria. The entomological inoculation rate in this area can exceed 300 infectious bites per year<sup>30</sup>. After informed consent was obtained, 144 male individuals aged 12–35 years were entered into the study at the beginning of the high-transmission season in April 1997. Detectable parasitaemia was eradicated in 143 of the 144 participants with quinine sulfate (10 mg kg<sup>-1</sup> twice daily for 3 days) and doxycycline (100 mg twice daily for 7 days). One volunteer remained parasitaemic during the week after treatment and was removed from the analysis, and five volunteers did not have available serum samples, thus our analytic sample size was *n* = 138. Immunological and epidemiological analyses of this cohort have been reported elsewhere<sup>14,29,31,32</sup>.

**Malaria assessment.** Thick and thin blood smears were obtained from each volunteer before treatment and then weekly for 18 weeks after treatment to quantify reinfection. Each smear was interpreted by two microscopists who were blinded to the clinical status of the participants and the mean of the two values was recorded.

**Entomology measurements.** The abundance of female *Anopheles* mosquitoes was measured weekly for 18 weeks in each volunteer's domicile using the daytime resting indoors (DRI) method<sup>33</sup> as previously described<sup>29</sup>.

**Blood collection.** Two weeks after treatment with quinine and doxycycline, volunteers donated 10 ml of blood into heparinized tubes. Within 4 h of collection, samples were centrifuged and plasma was aliquoted and stored at -80 °C for subsequent analysis.

**Clinical assays.** Sickle cell trait was determined by electrophoresis (Helena Laboratories).

### Selection of resistant and susceptible individuals for differential screening assays

Our overall purpose was to identify acquired differences in antibody repertoire that mediate resistance to parasitaemia. In our cohort, parasitaemia did not decline until after the age of two years (see Supplementary Fig. 1 from a previous study<sup>2</sup>). Any differences in parasitaemia between groups that were detectable in the first two years of life were unlikely to be due to differences in acquired antibody repertoire, as the children had made relatively little specific antibody by this age. Therefore, we wanted to ensure that the susceptibility to parasitaemia was similar (and high) between our resistant and susceptible groups in the first two years of life and then diverged after two years of age. The divergence after the age of two years was unlikely to be due to a constitutive (that is, genetic) feature and more likely to be due to a feature that is acquired (that is, antibody repertoire). Thus, we selected children for our two groups (resistant versus susceptible) to have similar levels of

parasitaemia in the first two years of life, and then to have very divergent levels of parasitaemia from the age of two to four years.

From our Tanzanian birth cohort, we excluded individuals with less than 9 of the total  $n = 18$  scheduled monthly blood smears collected between the age of 2 and 3.5 years, individuals with less than 200  $\mu\text{l}$  of plasma available from the plasma sample obtained at age 2 ( $\pm 2$  weeks), and individuals who were parasitaemic when the plasma sample from the age of 2 years ( $\pm 2$  weeks) was obtained. We then ordered individuals by rank on the basis of the mean parasite density on all blood films collected between the age of 2 and 3.5 years. This mean parasite density included the scheduled monthly blood smears as well as positive blood smears that were obtained during sick visits. Individuals from the low and high extremes of this distribution were chosen to comprise the 'resistant' ( $n = 12$ ) and 'susceptible' ( $n = 14$ ) groups. To minimize differential exposure as a possible confounder, resistant individuals were selected from those children who did not sleep under bed nets, whereas susceptible individuals were selected from those children who did sleep under bed nets. Selections were made with matching based on the village of residence and sex. Potential confounders examined included: haemoglobin phenotype, the presence of placental malaria, maternal age, birth season and number of previous pregnancies (Supplementary Table 1). By matching and demonstrating that potential non-immunological variables influencing resistance (for example, haemoglobin S (HbS)) were not differentially distributed between the resistant and susceptible groups, we substantially reduced the chance that these covariates were confounding the relationship between antibody specificities discovered and the outcome of resistance or susceptibility.

## Differential screening of whole blood-stage proteome

We constructed a *P. falciparum* blood-stage cDNA expression library prepared in a T7Select 10-3b vector (Invitrogen) using RNA prepared from freshly isolated parasites collected in our Tanzanian field site. This vector displays 5–15 copies of the cloned gene on the surface of phage capsids as a fusion with phage 10B protein.

We bound Immulon 4HB (Thermo Fisher Scientific) ELISA wells with 100  $\mu\text{l}$  of a 1:100 dilution of serum that was pooled from malaria-resistant children ( $n = 12$ ; see Supplementary Table 1) for 1 h at room temperature. Wells were washed five times with  $1\times$  TBST (10 mM Tris HCl, 150 mM NaCl, 0.05% Tween 20, pH 7.4) and blocked with 2% bovine serum albumin (BSA) in  $1\times$  TBST for 1 h at room temperature. Wells were probed with  $1\times 10^8$  phages in 100  $\mu\text{l}$  of  $1\times$  TBST and incubated for 1 h at room temperature. Unbound phages were removed and the wells were washed five times with  $1\times$  TBST. Bound phages were then eluted in 100  $\mu\text{l}$  of 5 M NaCl. Eluted phages were amplified and titered using BLT5403 bacteria according to the manufacturer's instructions. Amplified eluted phages were used as input phages for three additional rounds of positive selection.

After four rounds of positive selection, the titre of eluted phages was determined and adjusted to  $1\times 10^5$  per ml in  $1\times$  TBST buffer. For negative selection, we bound Immulon 4HB (Thermo Fisher Scientific) ELISA wells with 100  $\mu\text{l}$  of a 1:100 dilution of serum that was pooled from malaria-susceptible children ( $n = 14$ ; see Supplementary Table 1) for 1 h at room temperature. An aliquot of 100  $\mu\text{l}$  of the diluted phages (10,000 total phages) was added to the wells, wells were incubated for 1 h at room temperature and the unbound phages were collected. Unbound phages were transferred to an additional well coated with serum pooled from susceptible children, incubated for 1 h at room temperature and collected. This process was repeated a total of five times.

After negative selection, the titre of the eluted phages was determined and 100 individual plaques were isolated. Their cDNA inserts were amplified by PCR using the vectors T7SelectUP (5'-GGAGCTGTCGATTCCAGTC-3') and T7Select Down (5'-AACCCTCAAGACCCGTTTA-3') and the PCR products were sequenced.

## Expression and purification of PfGARP

We subcloned the open reading frame encoding amino acids 410–673 of PfGARP into pET30 (Novagen) and transformed the resulting plasmid into the expression host *E. coli* BL21(DE3) (Novagen). The pET30 vector encodes a His tag at both the amino and carboxy ends of the recombinant protein, thus facilitating purification by metal chelate chromatography. Transformants were grown in Terrific broth supplemented with 100  $\mu\text{g ml}^{-1}$  kanamycin, at 37 °C in a 10-l fermenter with oxygen sparging (10 l min<sup>-1</sup>) until an optical density at 600 nm ( $\text{OD}_{600}$ ) of 8.0 was reached. Isopropyl- $\beta$ -D-thiogalactopyranoside was added to a final concentration of 1 mmol l<sup>-1</sup>, and the culture was fed continuously with 0.3 g ml<sup>-1</sup> glucose, 0.09 g ml<sup>-1</sup> yeast extract at 50 ml h<sup>-1</sup> for 12 h. Cultures were collected by centrifugation and 750 g of wet cell paste was resuspended in 10 l of 10 mmol l<sup>-1</sup> potassium phosphate, 150 mmol l<sup>-1</sup> NaCl, 10 mmol l<sup>-1</sup> imidazole, 0.5% Tween 20 and 0.5% Triton X-100, pH 8.0 and lysed by high-pressure disruption at 20,000 psi (Microfluidics, Model 110-T). The lysate was clarified by tangential flow microfiltration (filter area 1 m<sup>2</sup>, pore size 1  $\mu\text{m}$ ; Millipore) and 8 l of clarified lysate was recovered. Protein purification was achieved by a 4-step process on BioPilot chromatography equipment (Pharmacia). In brief, clarified lysate was applied to a FineLine Pilot 35 (GE Healthcare) column containing 90 ml of Ni-NTA Superflow Resin (Novagen). The protein of interest was eluted with a stepped gradient containing increasing concentrations of imidazole. Fractions containing the protein of interest were pooled, adjusted to 400 mmol l<sup>-1</sup> ammonium sulfate, 10 mmol l<sup>-1</sup> DTT and further purified, by hydrophobic-interaction chromatography on a Fine Line Pilot 35 (GE Healthcare) column containing 150 ml of Source 15PHE (GE Healthcare). Recombinant proteins were eluted with a linear gradient of elution buffer (10 mmol l<sup>-1</sup> Tris, 1 mmol l<sup>-1</sup> DTT, 1 mmol l<sup>-1</sup> EDTA, pH 8.0). Fractions containing the protein of interest were pooled and further purified by anion-exchange chromatography on a Fine Line Pilot 35 (GE Healthcare) column containing 130 ml of MacroPrep High Q (BioRad). Recombinant proteins were eluted with a linear gradient of elution buffer (10 mmol l<sup>-1</sup> Tris, 1 mol l<sup>-1</sup> NaCl, 1 mmol l<sup>-1</sup> DTT, 1 mmol l<sup>-1</sup> EDTA, pH 8.0). Final purification was achieved by ceramic hydroxyapatite (CHT) chromatography on a FineLine Pilot 35 (GE Healthcare) column containing 70 ml of CHT type 1 (BioRad). Recombinant proteins were eluted with a linear gradient of elution buffer (500 mmol l<sup>-1</sup> potassium phosphate and 1 mmol l<sup>-1</sup> DTT, pH 7.4).

Purified recombinant protein, designated rPfGARP-A, was buffer-exchanged into 10 mmol l<sup>-1</sup> sodium phosphate, 0.05% Tween 20 and 3% sucrose, and concentrated to 500  $\mu\text{g ml}^{-1}$  by tangential flow ultrafiltration (filter area 50 cm<sup>2</sup>, pore size 5 kDa; Pall). rPfGARP was lyophilized at 500  $\mu\text{g}$  per vial and stoppered under nitrogen. Endotoxin levels were less than 2 EU per mg protein as determined by an FDA cleared assay (Lonza). Typical yields were over 50 mg rPfGARP per 750 g wet cell paste.

Notably, rPfGARP-A expresses immunorelevant epitopes, which generate functional polyclonal antibodies that block parasite growth and kill trophozoites (Fig. 1) and recognize native PfGARP by western blot (Extended Data Fig. 1).

## Parasite strains and culture

*P. falciparum* strains (3D7, Dd2 and D10) were obtained from MR4. Two parasite isolates from adults and two parasite isolates from children were collected from our Tanzanian field site and culture-adapted. The parasites were cultured in vitro according to the previously published methods, with minor modifications<sup>34</sup>. In brief, parasites were maintained in RPMI 1640 medium containing 25 mM HEPES, 5% human O+ erythrocytes, 5% Albumax II (Invitrogen), 24 mM sodium bicarbonate and 10  $\mu\text{g ml}^{-1}$  gentamycin at 37 °C with 5% CO<sub>2</sub>, 1% O<sub>2</sub> and 94% N<sub>2</sub>.

### Anti-PfGARP antisera

Mouse anti-PfGARP antisera were produced by immunization based on DNA, recombinant protein or mRNA. For DNA immunization, we subcloned the open reading frame encoding amino acids 410–673 of PfGARP into VR2001, transformed this into the host *E. coli* NovaBlue (Novagen), and purified the endotoxin-free plasmid (Endofree Giga, Qiagen). BALB/cj mice were immunized with 100 µg of plasmid (25 µg intramuscular injection in each hind leg and 50 µg intradermal injection at the base of the tail) followed by 50 µg intradermal injections at the base of the tail every two weeks for a total of four doses.

For protein immunization, we emulsified rPfGARP-A in an equal volume of TiterMax adjuvant (CytRx Corporation) and injected 50 µg of rPfGARP-A intraperitoneally at two-week intervals for a total of four doses.

For mRNA-based immunization, BALB/cj mice were immunized intradermally with 10 µg lipid-encapsulated mRNA (see below) encoding amino acids 410–673 of PfGARP every three weeks for a total of three doses.

### Affinity purification of anti-PfGARP antisera

To purify polyclonal mouse and human anti-PfGARP IgG, we coupled 6 mg of rPfGARP-A to one ml of NHS-activated Sepharose 4 Fast Flow (GE Health Sciences) according to the manufacturer's instructions. For mouse anti-PfGARP IgG, we used plasma pooled from rPfGARP-A immunized mice. For human anti-PfGARP IgG, we used plasma pooled from placental blood collected from women delivering in our Tanzanian birth cohort.

In brief, rPfGARP-A coupled resin was incubated with 600 µl of pooled mouse or human plasma diluted in 6 ml of phosphate-buffered saline (PBS). After extensive washing in PBS with 0.05% Tween 20, bound antibody was eluted in 0.1 M glycine, pH 2.5 and immediately neutralized with 1 M Tris HCl, pH 8. Eluted antibodies were buffer exchanged into PBS by dialfiltration in spin columns (Centricon) and sterilized before use in immunoblot and in vitro growth assays.

### Western blot

Parasite pellets were prepared by treatment of parasitized RBCs with 0.15% saponin in PBS, pH 7.4 on ice for 10 min, followed by centrifugation (3,000g, 5 min), resuspension in cold PBS and centrifugation (3,000g, 5 min). Alternatively, RBCs infected with mature-stage parasites were purified on a magnetic column and resuspended in distilled water (1:25 v/v) to lyse the RBCs, followed by centrifugation (3,000g, 5 min) to collect parasite pellets.

Parasite pellets or rPfGARP-A were dissolved in SDS sample-loading buffer with reducing agent (Bio-Rad) and heated to 95 °C for 10 min, and proteins were separated in 4–11% gradient SDS–PAGE gels. Separated proteins were transferred to nitrocellulose membranes, which were blocked in 5% milk PBS (pH 7.4) and 0.05% Tween 20 for 1 h. Membranes were probed with polyclonal anti-PfGARP or pre-immune mouse serum, detected by an anti-mouse IgG antibody conjugated to IRDyes and imaged on an LI-COR (Odyssey Imaging Systems).

### Growth inhibition assays

GIA were carried out with polyclonal anti-PfGARP or IgG monoclonal and polyclonal antibodies, control anti-fluorescein monoclonal antibodies, control mouse serum or IgG as described<sup>35,36</sup> with minor modifications. In brief, anti-PfGARP antibodies or controls were dialysed overnight in PBS, pH 7.4, heat-inactivated at 56 °C for 30 min and pre-incubated with human RBCs for 1 h before use in GIA assays. GIA assays were carried out using Dd2, 3D7, D10 or four newly adapted isolates of *P. falciparum* collected at our Tanzanian field site. Parasites were synchronized to the ring stage by treatment with 5% sorbitol<sup>37</sup> for three successive replication cycles and cultured to the ring stage. Parasites at 0.3–0.4% parasitaemia and 2% haematocrit were incubated

with antiserum or IgG, in a final volume of 100 µl in microtitre wells. Cultures were performed in triplicate with five replicates (comprising a total of 15 individual wells) prepared for each treatment condition. After 48 h, blood films were prepared from each replicate and stained with Giemsa. A microscopist blinded to the treatment conditions counted the RBCs that were infected with ring-stage parasites, and the results from the three wells were averaged. The relationship between the treatment group and the parasitaemia outcome of the five replicates was analysed by Mann–Whitney *U*-test.

In some GIA assays (Fig. 1d), parasites were plated at 0.08% parasitaemia and were incubated with antiserum, in a final volume of 100 µl in microtitre wells. Cultures were examined by microscopy daily for seven days. The medium (with appropriate antiserum) was changed daily. Cultures were performed in triplicate with five replicates (comprising a total of 15 individual wells) prepared for each treatment condition.

### Production of monoclonal antibodies and epitope mapping

We immunized BALB/cj mice intraperitoneally three times at two-week intervals with 25 µg of rPfGARP-A emulsified in TiterMax, and boosted with 25 µg of rPfGARP-A intravenously three days before fusion of splenocytes with P3X63Ag8.653 myeloma cells (ATCC) according to our published method<sup>33</sup>.

Hybridomas were cultured and cloned by limited dilutions. Hybridomas producing anti-PfGARP antibodies were screened and used for large-scale production of monoclonal antibodies.

The heavy- and light-chain variable regions of hybridoma clone 7899 (IgG1k) were sequenced, and recombinant plasmids were constructed and used for the production of recombinant monoclonal antibodies in HEK293 cells according to the manufacturer's protocols (Absolute Antibody). Recombinant monoclonal antibodies expressing the heavy- and light-chain variable regions from clone 7899 on a mouse IgG1 framework were purified by Protein A chromatography. Recombinant monoclonal antibodies expressing the heavy- and light-chain variable regions from clone 7899 on a mouse IgG1 Fab framework (monovalent) were purified by Ni-NTA chromatography.

For epitope mapping, a custom 15-mer peptide microarray was designed and printed. The array contained 264 different peptides that spanned the PfGARP-A sequence (amino acids 410–673). The peptides overlapped by a single amino acid and were printed in duplicate, framed by haemagglutinin control peptides. The array was probed with recombinant mAb7899 (red) and anti-HA (green) and imaged on a LI-COR Odyssey according to the manufacturer's protocol (PepperPrint).

### Mitochondrial membrane potential

Mitochondrial membrane potential was assessed with the dye JC-1, a cationic dye that exhibits membrane-potential-dependent accumulation in mitochondria. RBCs infected with ring-stage parasites from *P. falciparum* in vitro cultures were collected at 5–10% parasitaemia and incubated with anti-glycophorin A antibodies (Invitrogen) for 30 min at room temperature followed by Hoechst 33342 dye at 1 µg ml<sup>-1</sup>. JC-1 staining was performed at a final concentration of 2 µM for 30 min at 37 °C in the dark with constant agitation and analysed by flow cytometry.

### Caspase-activation assay

The activation of caspase-like proteases was quantified using a cell-permeable, fluorescein isothiocyanate (FITC)-conjugated pan-caspase inhibitor (FITC–VAD-FMK, Apostat, R&D Systems) which irreversibly binds and labels activated cysteine proteases. Antibody-treated *P. falciparum*-infected RBCs (treated with anti-PfGARP or control) were incubated with FITC–VAD-FMK, at a final concentration of 1%, 1 h before collection. Samples were washed with PBS to remove unbound reagent, and this was followed by staining with anti-glycophorin A antibodies (Invitrogen) and Hoechst 33342 dye (Thermo Fisher Scientific) as above. Samples were analysed by flow cytometry.

## TUNEL assay

Fragmentation of intracellular DNA in the cultured *P. falciparum* parasites was evaluated by TUNEL assay, using the APO-DIRECT Kit (BD Biosciences). Antibody-treated *P. falciparum*-infected RBCs (treated with anti-PfGARP or control) were collected, washed and stored in ice-cold 70% ethanol for at least 18 h before staining with 50 µl of DNA labelling solution, prepared as per the manufacturer's instructions. After incubation for about 1 h with the DNA labelling solution, samples were stained with anti-glycophorin A antibodies (Invitrogen) and Hoechst 33342 dye (Thermo Fisher Scientific) as above and analysed by flow cytometry.

## Lactate assay

The spent medium from 3D7 parasites incubated with recombinant anti-PfGARP monoclonal antibody or control recombinant anti-fluorescein in GIA assays was collected and assayed for lactate levels (lactate assay kit II, Sigma-Aldrich, MAK065) according to the manufacturer's protocol.

## Generation of 3D7-PfGARP KD and 3D7-PfGARP KO parasite lines

For 3D7-PfGARP KD parasites, approximately 100 µg of pRR203 was linearized with EcoRV, purified and co-transfected with 100 µg pRR183 into 3D7 parasites. Parasites were maintained on 500 nM anhydrotetracycline. One day after transfection, drug pressure was applied with 2.5 nM WR99210 and the PfDHODH inhibitor *N*-(3-chloro-4-methylphenyl)-5-methyl-2-(trifluoromethyl)[1,2,4]triazolo[1,5-a]pyrimidin-7-amine (MMV665874 or AD1) at 150 nM. Five days after transfection, AD1 selection was removed. Parasites were cloned by limiting dilution.

3D7-PfGARP KO parasites were made as above, with the exception that pRR248 was used as the homology-directed repair plasmid. pRR248 was linearized with AvrII, NotI and SapI and transfected with pRR183 into a strain of 3D7 parasites with episomal expression of spCas9. Only WR99210 drug pressure was applied after transfection.

For 3D7-PfGARP KD parasites, integration of the targeting construct was confirmed by PCR with oJDD1027/oJDD4507 (control), oJDD1027/oJDD2933 (integration) and oJDD4279/4280 (locus size). Tet aptamer size was confirmed by amplifying the aptamer with oJDD3560/oJDD44 and digesting the PCR fragment with PspOMI and KpnI. For 3D7-PfGARP KO parasites, integration of the targeting construct was similarly confirmed by PCR.

## Construction of PfGARP homology-directed repair plasmid.

To prevent homology-directed repair occurring between the spCas9-directed cut site and the 3' end of PfGARP, we synthesized caPfGARP, in which the last 438 bp of PfGARP were codon-altered. We amplified the synthesized gene with oJDD4506/oJDD3566, and the 500 bp preceding the codon-altered region from 3D7 genomic DNA with oJDD3563/oJDD4507. We amplified 500 bp from the 3' end of PfGARP for the 3' homology region with oJDD3561/oJDD3562 from 3D7 genomic DNA. We used PCR with splicing by overhang extension (SOE) to create a PfGARP 3'HR-EcoRV-PfGARP 5'HR-caPfGARP fusion. We cloned this fusion into pRR69<sup>38</sup> with NotI and NcoI to generate pRR203.

## Construction of PfGARP-targeting spCas9 vector and generation of knock-down parasite line.

A PfGARP-targeting guide was cloned into the U6 cassette of pBAM203<sup>38</sup> by PCR SOE. The U6 promoter with guide was amplified by oJDD3058/oJDD4088 and gRNA and U6 terminator with guide amplified with oJDD3059/oJDD4089. The cassette was cloned into pBAM203 with EcoRI and AvrII to generate pRR183. The 3D7 parasites were transfected with pRR183 and genome-integrated parasites were selected by serial dilution.

**Construction of PfGARP KO homology-directed repair plasmid.** To knock out PfGARP, we generated a cassette for double crossover that integrated into the 5' UTR of PfGARP and at the 3' end of the sequence coding for PfGARP. We amplified the 5' UTR of PfGARP from genomic DNA with oJDD4077/4979 and cloned it into a plasmid containing a cassette expressing the KAHRP signal sequence fused to nanoluciferase followed by a 2A skip peptide and the hDHFR selection marker. The 5' UTR of PfGARP was cloned upstream of the cassette with NotI/AflIII. The 3' homology region was amplified with oJDD5029/4083 and cloned downstream of the selection cassette with EcoRI/AvrII to generate pRR248.

## Immunofluorescence assays

Blood smears of asynchronous 3D7 strain parasite cultures were prepared, fixed in cold methanol for 15 min and probed with anti-PfGARP prepared by DNA vaccination, rabbit anti-PfMSP4 (obtained from MR4) or anti-rabbit glycophorin A diluted 1:200 in PBS, 5% BSA, pH 7.4. Blood smears were incubated with primary antibodies for 1 h at 25 °C, washed three times in PBS, 0.05% Tween 20 and incubated with goat anti-mouse IgG conjugated with Alexa Fluor 488 (Molecular Probes) and goat anti-rabbit IgG conjugated with Alexa Fluor 594 (Molecular Probes). Blood smears were incubated for 10 min in 1 µg ml<sup>-1</sup> DAPI (Sigma-Aldrich) to label nuclei and coverslipped with ProLong Gold anti-fade reagent (Invitrogen). Blood smears were imaged using a confocal microscope (Leica SP2, Leica Microsystems) equipped with a 100× oil-immersion objective, and sequential Z-sections of the infected RBC were collected. Immunofluorescence assays were also performed using anti-V5 monoclonal antibodies (Thermo-Fisher Scientific) and control IgG as described above.

To assess the colocalization of PfGARP with the membrane of the food vacuole, we probed parasites with both anti-PfGARP and anti-PfCRT, a protein which localizes to the food vacuole membrane<sup>39</sup>.

In some experiments, parasite-infected RBCs were incubated with primary antibodies before fixation and slide preparation to ensure that the methanol used for fixation did not permeabilize the RBC membrane.

## Transmission electron microscopy

To assess the effect of anti-PfGARP on parasite ultrastructure, we performed transmission electron microscopy on parasites after a 24-h incubation with anti-PfGARP or control antibodies. 3D7 strain parasites were grown to high parasitaemia (10%) consisting of predominantly trophozoites. Parasites were incubated with anti-PfGARP prepared by DNA or rPfGARP-A vaccination at 10% serum concentration for 24 h at 37 °C. Pre-immune mouse serum at 10% serum concentration was used as a negative control.

Parasites were washed three times in 1× PBS, and were fixed for 30 min at 4 °C with 2% glutaraldehyde and 1% paraformaldehyde in 0.1 M sodium cacodylate buffer. Samples were dehydrated, embedded in Epon (EMS), sectioned on an ultra-microtome, counterstained for 10 min in 5% aqueous uranyl acetate and examined on a Philips CM10 electron microscope.

For immunoelectron microscopy, we performed live-cell staining followed by fixation. Parasitized RBCs were blocked for 1 h at 25 °C in 1× PBS containing 2% BSA. Samples were incubated with anti-PfGARP prepared by DNA or rPfGARP-A vaccination (diluted 1:200 in PBS) for 3 h at 25 °C. Pre-immune mouse serum was used as a negative control. The samples were washed three times in 1× PBS and probed with gold-conjugated anti-mouse antibodies for 1 h at 25 °C at 1:2 dilution (Invitrogen). Samples were washed three times in 1× PBS, fixed and processed as described above.

## Assessment of food vacuole integrity

We further evaluated the effect of anti-PfGARP antibodies on food vacuole integrity by confocal microscopy using the calcium-binding

dye Fluo-4 AM (a cell-permeable calcium-sensing dye that fluoresces green when bound with  $\text{Ca}^{2+}$ ), which specifically labels the food vacuole. Ring-stage 3D7 parasites were incubated with culture medium (negative control), 1  $\mu\text{M}$  chloroquine (positive control) or anti-PfGARP prepared by rPfGARP-A immunization for 24 h. Parasites were washed with 1 $\times$  PBS three times and incubated with Fluo-4 AM at a final concentration of 2  $\mu\text{M}$  and DAPI for 30 min at 37 °C. The parasites were washed with 1 $\times$  PBS and observed under a fluorescent microscope. Under normal conditions,  $\text{Ca}^{2+}$  ions sequester inside the food vacuole of the parasite, which results in a punctate staining pattern of Fluo-4 AM. Treatment with chloroquine or anti-PfGARP disrupted the food vacuole leading to dispersion of  $\text{Ca}^{2+}$  ions into the cytosol of the parasite and resulted in a diffuse staining pattern of Fluo-4 AM.

### Serial block-face scanning electron microscopy

To further assess the effect of anti-PfGARP on parasite ultrastructure, we performed SBF-SEM on parasite-infected RBCs that had been treated with anti-PfGARP or pre-immune antiserum. Ring-stage 3D7 strain parasites were grown to 5% parasitaemia and incubated with anti-PfGARP (prepared by DNA vaccination) or pre-immune serum (10% final serum concentration) for 30 h at 37 °C. Parasites were washed three times in 1 $\times$  PBS and fixed for 1 h at 4 °C with 2% glutaraldehyde in 0.1 M sodium cacodylate buffer containing 1 mM  $\text{CaCl}_2$  and 1 mM  $\text{MgCl}_2$ . Samples were washed five times with sodium cacodylate buffer. Samples were incubated at 4 °C for 1 h with 1% osmium tetroxide and 1.5% potassium ferrocyanide in sodium cacodylate buffer followed by five washes with deionized water. Samples were incubated in 1% aqueous thiocarbonylhydrazide for 20 min followed by five washes with deionized water. Samples were incubated in 1% aqueous osmium tetroxide for 30 min, followed by overnight incubation at 4 °C in 1% uranyl acetate in 70% ethanol followed by five washes with deionized water. Samples were finally incubated in 0.2% aqueous lead citrate for 30 min before being dehydrated, treated with propylene oxide and embedded in Epon resin (EMS). Once cured, samples were cut and mounted on a 6.6-mm specimen mount with conductive silver epoxy (MG Chemicals). Specimens were coated with gold palladium using an Emitech K550 sputter coater before being sectioned and imaged with a Thermo Apreo Volume Scope scanning electron microscope in high-vacuum conditions. Acquired images were processed and the final three-dimensional reconstruction was performed with Amira 2019.2 software.

### Processing of PfGARP

PfGARP encodes a predicted N-terminal signal sequence or transmembrane region (amino acids 1–22) and an appropriately located PEXEL motif (amino acids 48–52). To determine whether parasites process and cleave the PEXEL motif, we probed western blots of parasite extracts and rPfGARP-A using peptide-specific antisera generated against peptides that flank the PEXEL motif (amino acids 31–48 and 504–522).

### Anti-PfGARP antibody assays

Initial, confirmatory antibody assays were performed with rPfGARP-coated ELISA plates according to our published methods. To measure IgG anti-rPfGARP antibody levels in the Kenyan cohort; we developed a bead-based assay according to our published methods<sup>40</sup>. In brief, 100  $\mu\text{g}$  of rPfGARP-A or 100  $\mu\text{g}$  of BSA was conjugated to  $1.25 \times 10^7$  microspheres (Luminex), and conjugated rPfGARP and BSA beads were pooled and lyophilized in single-use aliquots. Reconstituted beads were incubated for 30 min at 37 °C with human plasma samples at 1:80 dilution in Assay Buffer E (ABE; PBS pH 7.4 containing 0.1% BSA, 0.05% Tween 20 and 0.05% sodium azide) in microtitre filter-bottom plates (Millipore). Beads were washed three times in ABE by vacuum filtration and incubated for 30 min at 37 °C with biotinylated anti-human IgG (Pharmingen) diluted 1:1,000 in ABE. Beads were washed three times in ABE by vacuum filtration and incubated for 10 min at 37 °C with phycoerythrin-conjugated streptavidin (Pharmingen) diluted

1:500 in ABE. Beads were washed three times in ABE by vacuum filtration, resuspended in ABE and analysed on a BioPlex 200 multi-analyte analyser. Fluorescence values for BSA beads were subtracted from rPfGARP beads. The cut-off for detectable anti-PfGARP antibody levels was defined as fluorescence values greater than the mean + 2 s.d. fluorescence level of 22 healthy North American adults.

To measure IgG anti-rPfGARP antibody levels in the Tanzanian cohort, we performed bead-based assays using amino acids 23–673 of PfGARP expressed and purified from COS-7 cells as the target antigen. We expressed and purified amino acids 23–673 of PfGARP (excluding initial signal sequence or transmembrane domain) in a eukaryotic expression system (COS-7 cells) according to our published methods<sup>41–43</sup>. In brief, the coding sequence for amino acids 23–673 of PfGARP was PCR-amplified with primers encoding BamHI and EcoRI restriction sites, gel-purified, digested with BamHI and EcoRI, and ligated into BamHI- and EcoRI-digested vector pAdEx<sup>41–43</sup>. The integrity of the PfGARP construct was verified by sequencing on both strands. Transfection of COS-7 cells, expression, extraction and immobilization of recombinant PfGARP protein and control AdEx protein on the surface of BioPlex beads have been described in detail in our previous publications<sup>41–43</sup>. Immobilization of recombinant PfGARP on beads was verified by reactivity with mouse anti-PfGARP antibodies. PfGARP and AdEx-only beads were incubated for 30 min at 37 °C with human plasma samples at 1:80 dilution in ABE (PBS pH 7.4 containing 0.1% BSA, 0.05% Tween 20 and 0.05% sodium azide) in microtitre filter-bottom plates (Millipore). Beads were washed three times in ABE by vacuum filtration and incubated for 30 min at 37 °C with biotinylated anti-human IgG (Pharmingen) diluted 1:1,000 in ABE. Beads were washed three times in ABE by vacuum filtration and incubated for 10 min at 37 °C with phycoerythrin-conjugated streptavidin (Pharmingen) diluted 1:500 in ABE. Beads were washed three times in ABE by vacuum filtration, resuspended in ABE and analysed on a BioPlex 200 multi-analyte analyser. Fluorescence values for AdEx beads were subtracted from rPfGARP beads. The cut-off for detectable anti-PfGARP antibody levels was defined as fluorescence values for rPfGARP beads exceeding the value for AdEx beads.

### Statistical analyses of cohort studies

**Tanzanian birth cohort.** To assess the relationship between anti-PfGARP antibody responses and resistance to clinical malaria outcomes, we developed GEE-based repeated measures models with antibody levels as a continuous variable (SAS v.9.3). These models were used to evaluate the relationship between anti-PfGARP antibody levels (log-transformed) and the risk of malaria outcomes.

Potential confounders and effect modifiers—including haemoglobin phenotype, birthweight and transmission season at birth—were evaluated with the two-sided fixed-effect test and retained in the model if their *P* value was less than 0.1 or their inclusion altered the  $\beta$  coefficient for the anti-PfGARP term by more than 10%. Only haemoglobin phenotype met the pre-specified criteria for inclusion ( $P < 0.1$ ). We report both the unadjusted results and the model adjusted for haemoglobin phenotype.

**Kenyan cohort.** To assess the relationship between anti-PfGARP antibody responses and resistance to *P. falciparum* parasitaemia, we developed GEE-based repeated measures models using JMP v.10. We evaluated the relationship between detectable anti-PfGARP IgG antibodies and parasite density measured on 18 post-treatment blood films. We assessed several potential confounders and effect modifiers including age, week of follow-up, exposure to *Anopheles* mosquitoes and haemoglobin phenotype using the two-sided fixed-effect test. Variables, including the week of monitoring, were retained in the model if their *P* value was less than 0.1 or they changed the parameter estimate for the antibody of interest by >10%. Age, exposure and haemoglobin phenotype were retained for face validity, although they did not meet the

# Article

pre-specified criteria for inclusion, and PfGARP antibodies remained a significant predictor of parasite density with their exclusion.

## Production of PfGARP-A mRNA

mRNAs were produced as previously described<sup>44</sup> using T7 RNA polymerase (Megascript, Ambion) on a linearized plasmid encoding codon-optimized<sup>45</sup> PfGARP-A. mRNAs were transcribed to contain 101 nucleotide-long poly(A) tails. One-methylpseudouridine (m1Ψ)-5'-triphosphate (TriLink) instead of UTP was used to generate modified nucleoside-containing mRNA. RNAs were capped using the m7G capping kit with 2'-O-methyltransferase (ScriptCap, CellScript) to obtain cap1. mRNA was purified by FPLC (Akta Purifier, GE Healthcare) as described<sup>46</sup>. All mRNAs were analysed by denaturing or native agarose gel electrophoresis and were stored frozen at -20 °C.

## Encapsulation of mRNA in LNPs

Poly(C) RNA (Sigma-Aldrich) and FPLC-purified m1Ψ-containing mRNAs were encapsulated in LNPs using a self-assembly process in which an aqueous solution of mRNA at pH 4.0 is rapidly mixed with a solution of lipids dissolved in ethanol<sup>47</sup>. LNPs used in this study were similar in composition to those described previously<sup>48</sup>, containing an ionizable cationic lipid (proprietary to Acuitas)/phosphatidylcholine/cholesterol/PEG lipid (50:10:38.5:1.5 mol/mol) and were encapsulated at an RNA to total lipid ratio of around 0.05 (w/w). They had a diameter of around 80 nm as measured by dynamic light scattering using a Zetasizer Nano ZS (Malvern Instruments). mRNA LNPs were stored at -80 °C at a concentration of mRNA of around 1 μg μl<sup>-1</sup>.

## Studies of *Aotus* monkey vaccination with mRNA LNPs

We immunized  $n = 5$  monkeys with 50 μg of PfGARP-A-mRNA LNPs, and  $n = 4$  monkeys with 50 μg of poly(C)-RNA LNPs, intradermally on four sites of the shaved back. Monkeys received 3 doses at weeks 0, 3 and 6. Before each immunization, serum samples were obtained for antibody assays. At week 9, monkeys were challenged by intravenous injection with  $1 \times 10^4$  RBCs infected with blood-stage *P. falciparum* FVO strain parasites, followed by daily blood films. Antibody assays were performed with PfGARP-A-coated beads according to our published methods<sup>40</sup> using a biotin-conjugated anti-monkey IgG antibody (Invitrogen) for detection of bound anti-PfGARP. Monkeys were monitored daily by blood samples from day 4 after challenge to quantify parasitaemia and haemoglobin concentration. Monkeys with parasitaemia greater than 7.5%, haematocrit lower than 25% or that exhibited signs of illness (fever, immobility, decreased food intake and so on) were treated with oral mefloquine in accordance with our animal protocol.

## Vaccination of *Aotus* monkeys with rPfGARP-A

We immunized  $n = 4$  monkeys intradermally with 50 μg of recombinant, *E. coli*-produced PfGARP-A (amino acids 410–673) emulsified in Ribi adjuvant, and  $n = 5$  monkeys with Ribi adjuvant alone as control. Monkeys received 3 doses at weeks 0, 3 and 6. Before each immunization, samples of serum were obtained for antibody assays. At week 9, monkeys were challenged by intravenous injection with  $1 \times 10^4$  RBCs infected with blood-stage *P. falciparum* FVO strain parasites, followed by daily blood films. Antibody assays were performed with PfGARP-A coated beads according to our published methods<sup>40</sup> using biotin-conjugated anti-monkey IgG antibody (Invitrogen) for detection of bound anti-PfGARP. Monkeys were monitored daily by blood samples from day 4 post-challenge to quantify parasitaemia and haemoglobin concentration. Monkeys with parasitaemia greater than 7.5%, haematocrit lower than 25% or that exhibited signs of illness (fever, immobility, decreased food intake and so on) were treated with oral mefloquine in accordance with our animal protocol.

## Reporting summary

Further information on research design is available in the Nature Research Reporting Summary linked to this paper.

## Data availability

Source Data for Extended Data Figs. 5 and 9 are provided with the paper. The DNA sequence for PfGARP is available in PlasmoDB ([www.plasmodb.org](http://www.plasmodb.org)) under the gene ID PF3D7\_0113000. All other relevant data are available within the manuscript and its Supplementary Information.

27. Ellman, R., Maxwell, C., Finch, R. & Shayo, D. Malaria and anaemia at different altitudes in the Muheza district of Tanzania: childhood morbidity in relation to level of exposure to infection. *Ann. Trop. Med. Parasitol.* **92**, 741–753 (1998).
28. Kabyemela, E. R., Fried, M., Kurtis, J. D., Mutabingwa, T. K. & Duffy, P. E. Decreased susceptibility to *Plasmodium falciparum* infection in pregnant women with iron deficiency. *J. Infect. Dis.* **198**, 163–166 (2008).
29. Kurtis, J. D., Lanar, D. E., Opollo, M. & Duffy, P. E. Interleukin-10 responses to liver-stage antigen 1 predict human resistance to *Plasmodium falciparum*. *Infect. Immun.* **67**, 3424–3429 (1999).
30. Beier, J. C. et al. *Plasmodium falciparum* incidence relative to entomologic inoculation rates at a site proposed for testing malaria vaccines in western Kenya. *Am. J. Trop. Med. Hyg.* **50**, 529–536 (1994).
31. Friedman, J. F. et al. Malaria is related to decreased nutritional status among male adolescents and adults in the setting of intense perennial transmission. *J. Infect. Dis.* **188**, 449–457 (2003).
32. Gourley, I. S., Kurtis, J. D., Kamoun, M., Amon, J. J. & Duffy, P. E. Profound bias in interferon-γ and interleukin-6 allele frequencies in western Kenya, where severe malarial anemia is common in children. *J. Infect. Dis.* **186**, 1007–1012 (2002).
33. Gunasekaran, K., Jambulingam, P., Sadanandane, C., Sahu, S. S. & Das, P. K. Reliability of light trap sampling for *Anopheles fluviatilis*, a vector of malaria. *Acta Trop.* **58**, 1–11 (1994).
34. Trager, W. & Jensen, J. B. Human malaria parasites in continuous culture. *Science* **193**, 673–675 (1976).
35. Bejon, P. et al. Effect of the pre-erythrocytic candidate malaria vaccine RTS,S/AS01E on blood stage immunity in young children. *J. Infect. Dis.* **204**, 9–18 (2011).
36. Malkin, E. M. et al. Phase 1 clinical trial of apical membrane antigen 1: an asexual blood-stage vaccine for *Plasmodium falciparum* malaria. *Infect. Immun.* **73**, 3677–3685 (2005).
37. Lambros, C. & Vanderberg, J. P. Synchronization of *Plasmodium falciparum* erythrocytic stages in culture. *J. Parasitol.* **65**, 418–420 (1979).
38. Rudloff, R. M., Kraemer, S., Strelva, V. A. & Dvorin, J. D. An essential contractile ring protein controls cell division in *Plasmodium falciparum*. *Nat. Commun.* **10**, 2181 (2019).
39. Pulcini, S. et al. Mutations in the *Plasmodium falciparum* chloroquine resistance transporter, PfCRT, enlarge the parasite's food vacuole and alter drug sensitivities. *Sci. Rep.* **5**, 14552 (2015).
40. Cham, G. K. et al. A semi-automated multiplex high-throughput assay for measuring IgG antibodies against *Plasmodium falciparum* erythrocyte membrane protein 1 (PFEMP1) domains in small volumes of plasma. *Malar. J.* **7**, 108 (2008).
41. Oleinikov, A. V. et al. High throughput functional assays of the variant antigen PFEMP1 reveal a single domain in the 3D7 *Plasmodium falciparum* genome that binds ICAM1 with high affinity and is targeted by naturally acquired neutralizing antibodies. *PLoS Pathog.* **5**, e1000386 (2009).
42. Oleinikov, A. V. et al. Effects of sex, parity, and sequence variation on seroreactivity to candidate pregnancy malaria vaccine antigens. *J. Infect. Dis.* **196**, 155–164 (2007).
43. Oleinikov, A. V. et al. A plasma survey using 38 PFEMP1 domains reveals frequent recognition of the *Plasmodium falciparum* antigen VAR2CSA among young Tanzanian children. *PLoS One* **7**, e31011 (2012).
44. Pardi, N., Muramatsu, H., Weissman, D. & Karikó, K. In vitro transcription of long RNA containing modified nucleosides. *Methods Mol. Biol.* **969**, 29–42 (2013).
45. Thess, A. et al. Sequence-engineered mRNA without chemical nucleoside modifications enables an effective protein therapy in large animals. *Mol. Ther.* **23**, 1456–1464 (2015).
46. Weissman, D., Pardi, N., Muramatsu, H. & Karikó, K. HPLC purification of in vitro transcribed long RNA. *Methods Mol. Biol.* **969**, 43–54 (2013).
47. Maier, M. A. et al. Biodegradable lipids enabling rapidly eliminated lipid nanoparticles for systemic delivery of RNAi therapeutics. *Mol. Ther.* **21**, 1570–1578 (2013).
48. Jayaraman, M. et al. Maximizing the potency of siRNA lipid nanoparticles for hepatic gene silencing in vivo. *Angew. Chem.* **51**, 8529–8533 (2012).

**Acknowledgements** We thank MOMS project staff for their efforts in collecting clinical data, processing samples and interpreting malarial blood smears, and we thank the study participants and their families. This work was supported by grants from the US NIH (R01-AI076353, R01-AI127699 and R01-AI110699) and an internal Rhode Island Hospital Research Pilot Award grant to J.D.K.; grants from the US NIH (R01-AI52059) and the Bill & Melinda Gates Foundation (grant no. 1364) to P.E.D.; the Intramural Research Program of the NIH National Institute of Allergy and Infectious Diseases (NIAID), NIH grant R01-AI092120 and Florida Atlantic University start-up funds to A.V.O.; NIH grant R37-AI50234 to D.A.F.; and NIH grants R01-AI145941 and R01-AI102907 to J.D.D. We also acknowledge research core services provided by the Rhode Island Hospital imaging core (G. Hovanesian), the Leduc Biomaging Facility (G. Williams) and core services supported by the COBRE Center for Cancer Research Development (P20GM103421). The Thermo Apreo Volume Scope scanning electron microscope that was used for the serial block-face imaging was purchased with a high-end instrumentation grant from the Office of the Director at the NIH (S10 ODO23461). L.L., S. O.-G., M.F. and P.E.D. are supported by the Intramural Research Program of the NIAID.

**Author contributions** J.D.K., D.K.R., M.F. and P.E.D. conceived and supervised the study. J.D.K., P.E.D., M.F., J.F.F., S.P., C.B.M., D.A.F., D.K.R. and A.D.M. analysed the data and/or drafted the

text. D.K.R., A.D.M., A. Jnawali, J.Z., A. Jha, G.C.-K., B.S., C.E.N., N.H., S.P.-T. and L.B. contributed to parasite killing assays. D.K.R., J.Z., A.D.M., G.J., D.A.F., A.M. and N.F.G. contributed to imaging studies. P.E.D., M.F., J.D.K. and E.K. contributed to field-based data collection. P.E.D., M.F., S.P., J.F.F., A.V.O., O.C., J.D.K. and J.M. contributed to epidemiological analyses. R.M.R. and J.D.D. contributed to genetic modification of parasites. N.P., D.W., B.L.M. and Y.K.T. contributed to mRNA-based vaccine design and production. D.K.R., L.L., S.O.-G., M.F., P.E.D. and J.D.K. contributed to non-human primate studies.

**Competing interests** The work presented in this manuscript has been submitted in partial support of patent no. US10,213,502 B2 (filed 26 May 2017) on the use of PfGARP as a vaccine,

on which the authors J.D.K., D.K.R., J.F.F., M.F. and P.E.D. are named inventors. The remaining authors declare no competing interests.

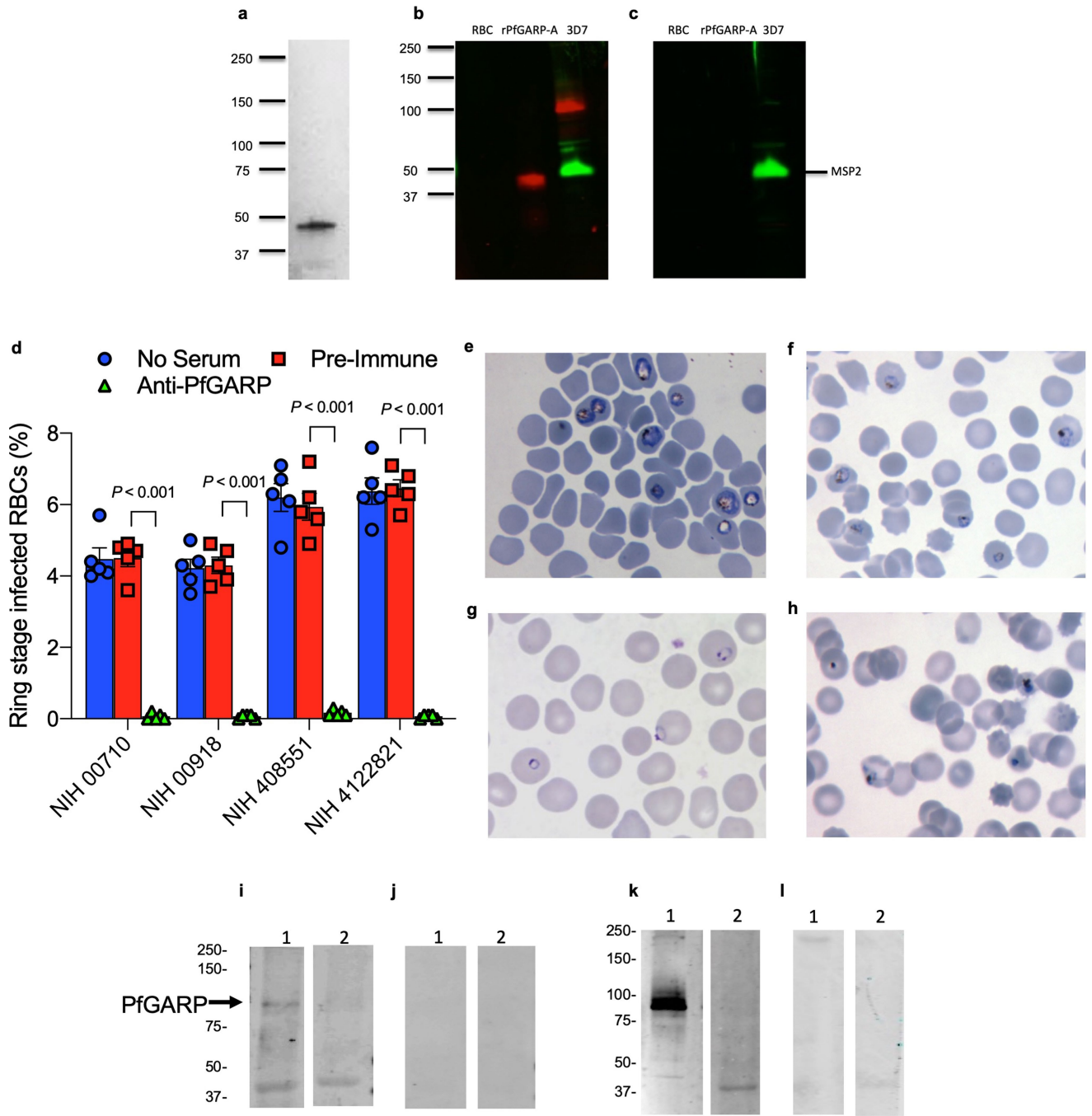
**Additional information**

**Supplementary information** is available for this paper at <https://doi.org/10.1038/s41586-020-2220-1>.

**Correspondence and requests for materials** should be addressed to J.D.K.

**Peer review information** *Nature* thanks Peter Preiser and the other, anonymous, reviewer(s) for their contribution to the peer review of this work.

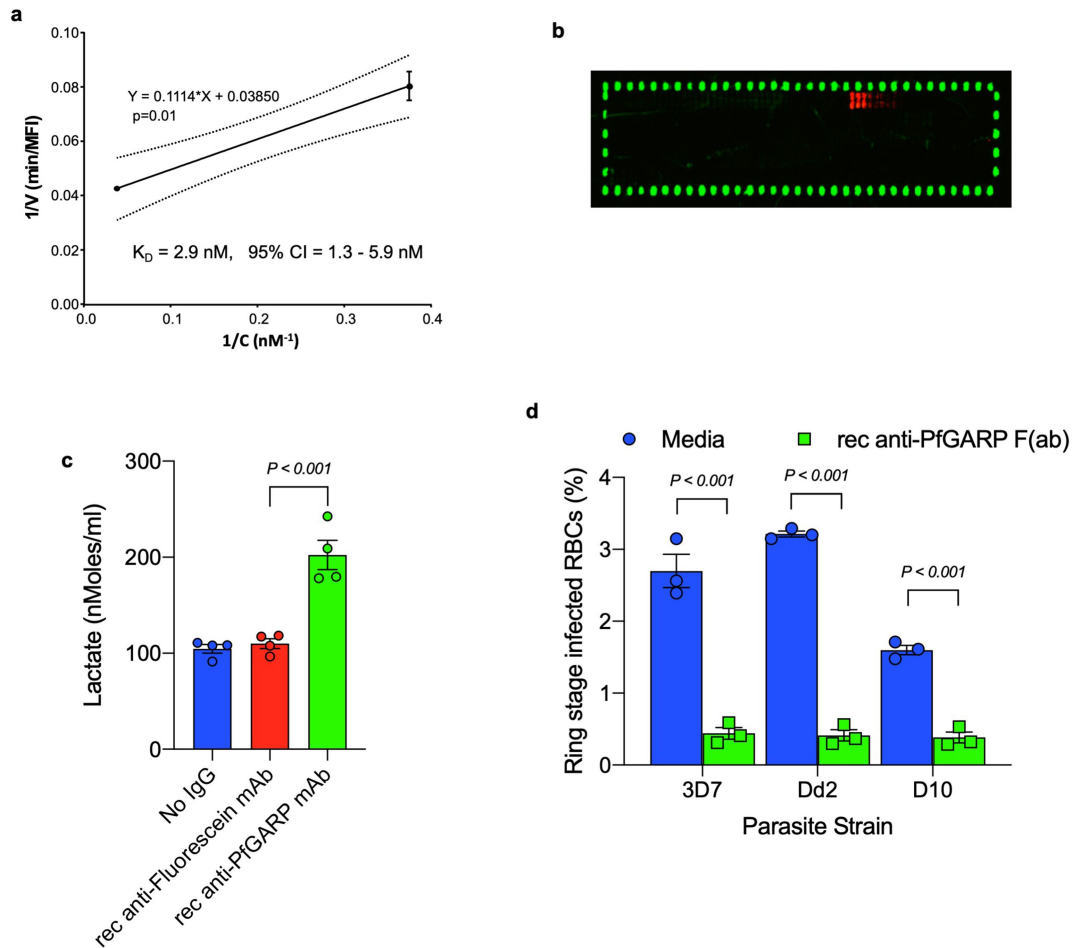
**Reprints and permissions information** is available at <http://www.nature.com/reprints>.



Extended Data Fig. 1 | See next page for caption.

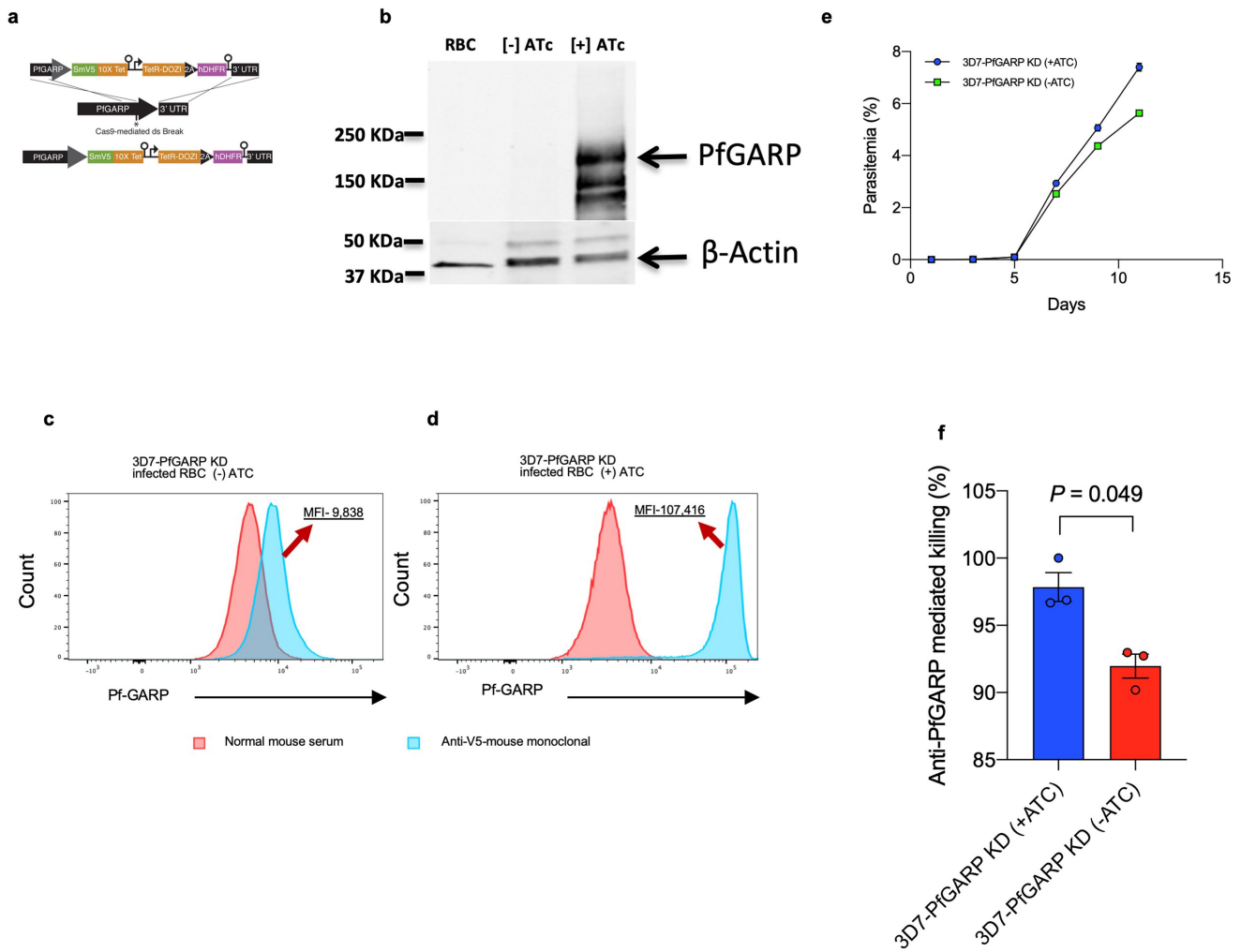
**Extended Data Fig. 1 | Expression of PfGARP, killing of parasites by anti-PfGARP and purification of anti-PfGARP antibodies.** **a**, SDS-PAGE gel of purified rPfGARP-A (250 ng). **b, c**, We analysed rPfGARP-A, as well as extracts prepared from uninfected RBCs and 3D7 trophozoite-infected RBCs by western blot. **b**, Blots were probed with mouse polyclonal anti-PfGARP-A serum (generated by plasmid immunization) and with anti-MSP2 (rabbit polyclonal serum), which were detected with anti-mouse IgG (red) and anti-rabbit IgG (green). **c**, Blots were probed with pre-immune mouse serum and anti-MSP2 (rabbit polyclonal serum), detected with anti-mouse IgG (red) and anti-rabbit IgG (green). Data in **a–c** are representative of five independent experiments. **d**, GIAs performed on parasites collected from our field site in Muheza, Tanzania, after short-term adaptation to the culture. Assays were performed using polyclonal anti-PfGARP-A antibodies generated by immunizing mice with recombinant protein. Ring-stage malaria parasites from adults (NIH 00710 and NIH 00918) or children (NIH 408551 and NIH 4122821) were cultured in the presence of anti-PfGARP mouse serum at a 1:10 dilution. Negative controls were no antiserum (blue) and pre-immune mouse serum (red). Parasites were cultured for 48 h at 37 °C and ring-stage and early-trophozoite-stage parasites were counted by microscopy. Data are mean  $\pm$  s.e.m. of five biologically independent replicates. *P* values were calculated by two-sided non-parametric

Mann–Whitney *U*-test. Data are representative of five independent experiments. **e–h**, 3D7 *P. falciparum* parasites were synchronized to the ring stage and plated at 5% parasitaemia in the presence of pre-immune (**e, g**) and anti-rPfGARP-A (**f, h**) mouse serum at a 1:10 dilution. Parasites were cultured for 24 h (**e, f**) or 48 h (**g, h**), stained with Giemsa and photographed by light microscopy. Images in **e–h** are representative of three independent experiments. **i–l**, Purification of anti-PfGARP antibodies from human (**i, j**) and mouse (**k, l**) serum. Serum was affinity-purified using PfGARP-A coupled to sepharose beads. The specificity of the purified anti-PfGARP antibodies was determined by western blot on extracts prepared from unsynchronized 3D7 parasite-infected RBCs. In all panels: lane 1, infected RBCs extracted in RIPA buffer; lane 2, uninfected RBCs extracted in RIPA buffer. Blots in **i, j** were probed with anti-PfGARP purified from serum that was pooled from adults living in a holoendemic area of Tanzania ( $2 \mu\text{g ml}^{-1}$ ) (**i**), or with immunoglobulin from malaria-naive adults ( $2 \mu\text{g ml}^{-1}$ ) (**j**). Blots in **k, l** were probed with anti-PfGARP purified from serum that was prepared from PfGARP-A-immunized mice ( $10 \mu\text{g ml}^{-1}$ ) (**k**), or immunoglobulin from malaria-naive mice ( $10 \mu\text{g ml}^{-1}$ ) (**l**). Blots in **i–l** are representative of two biologically independent experiments.



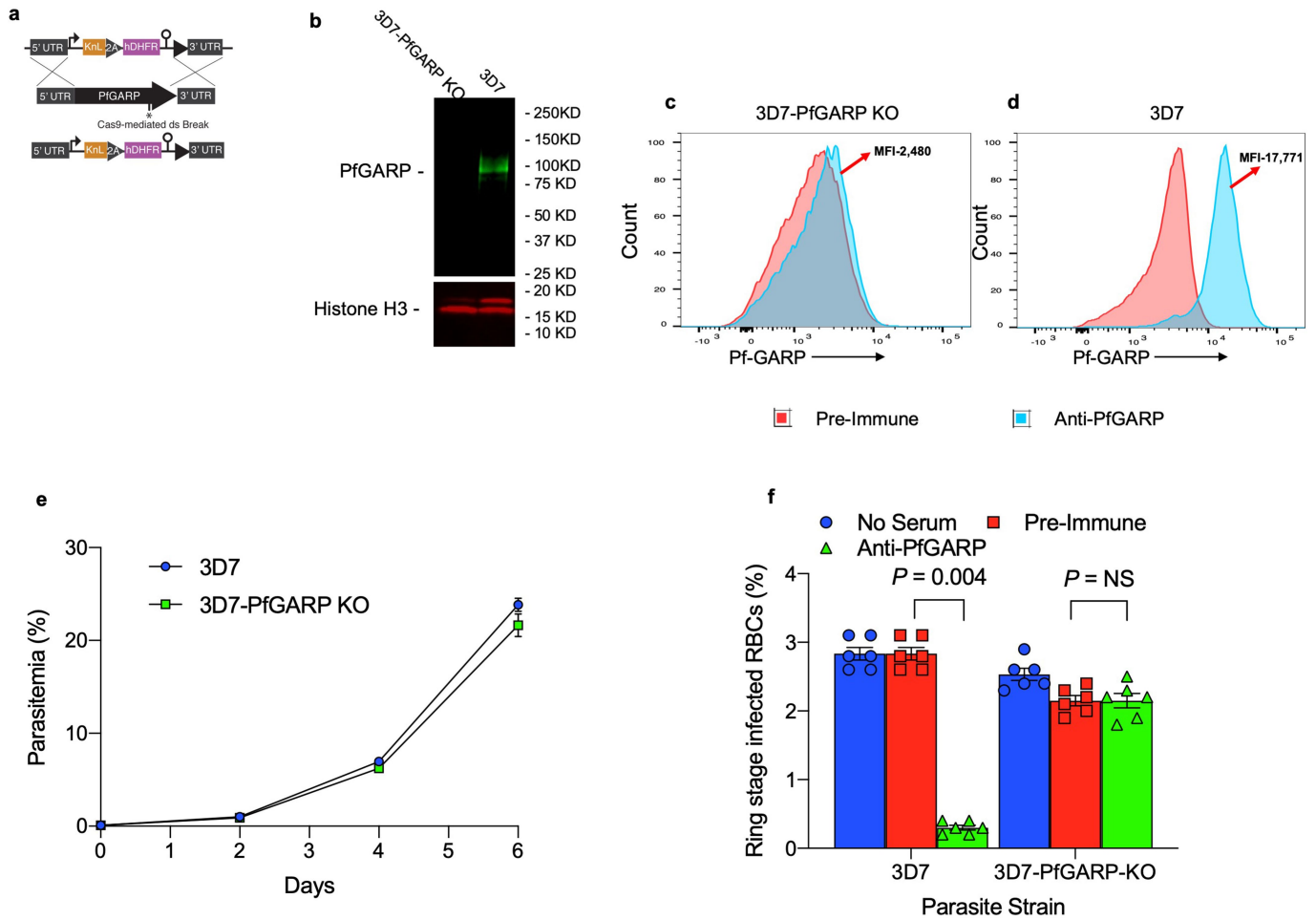
**Extended Data Fig. 2 | Characterization of recombinant monoclonal anti-PfGARP.** **a.** The kinetics of binding between the recombinant monoclonal antibody mAb7899 and PfGARP-A were measured at two antibody concentrations. For each concentration, two biologically independent replicates were performed. The experiment was performed twice and the data were pooled. The dashed lines represent the 95% CI. Error bars represent s.d. The formula is a linear regression. *C*, concentration of biotinylated recombinant mAb7899; MFI, median fluorescence intensity; *V*, initial velocity of binding. **b.** Epitope mapping of recombinant mAb7899. We printed a custom 15-mer-peptide microarray containing 264 different peptides that spanned the PfGARP-A sequence (amino acids 410–673). The peptides overlapped by a single amino acid and were printed in duplicate, framed by haemagglutinin (HA) control peptides. The array was probed with recombinant mAb7899 (red)

and anti-HA (green) and imaged on an LI-COR Odyssey. **c.** RBCs infected with ring-stage 3D7 parasites were cultured in the presence of medium alone, recombinant anti-PfGARP monoclonal antibody or recombinant anti-fluorescein. Parasites were cultured for 48 h at 37 °C and the levels of lactate were measured in the culture supernatant. Data are mean ± s.e.m. of four biologically independent replicates. The *P* value was calculated by non-parametric two-sided Mann–Whitney *U*-test. **d.** RBCs infected with ring-stage 3D7, D10 or Dd2 parasites were cultured in the presence of medium alone or recombinant anti-PfGARP Fab antibody (1 mg ml<sup>-1</sup>) for 48 h at 37 °C, and ring-stage or early-trophozoite-stage parasites were counted by microscopy. Data are mean ± s.e.m. of three biologically independent replicates. *P* values were calculated by non-parametric two-sided Mann–Whitney *U*-test. Data are representative of two independent experiments.



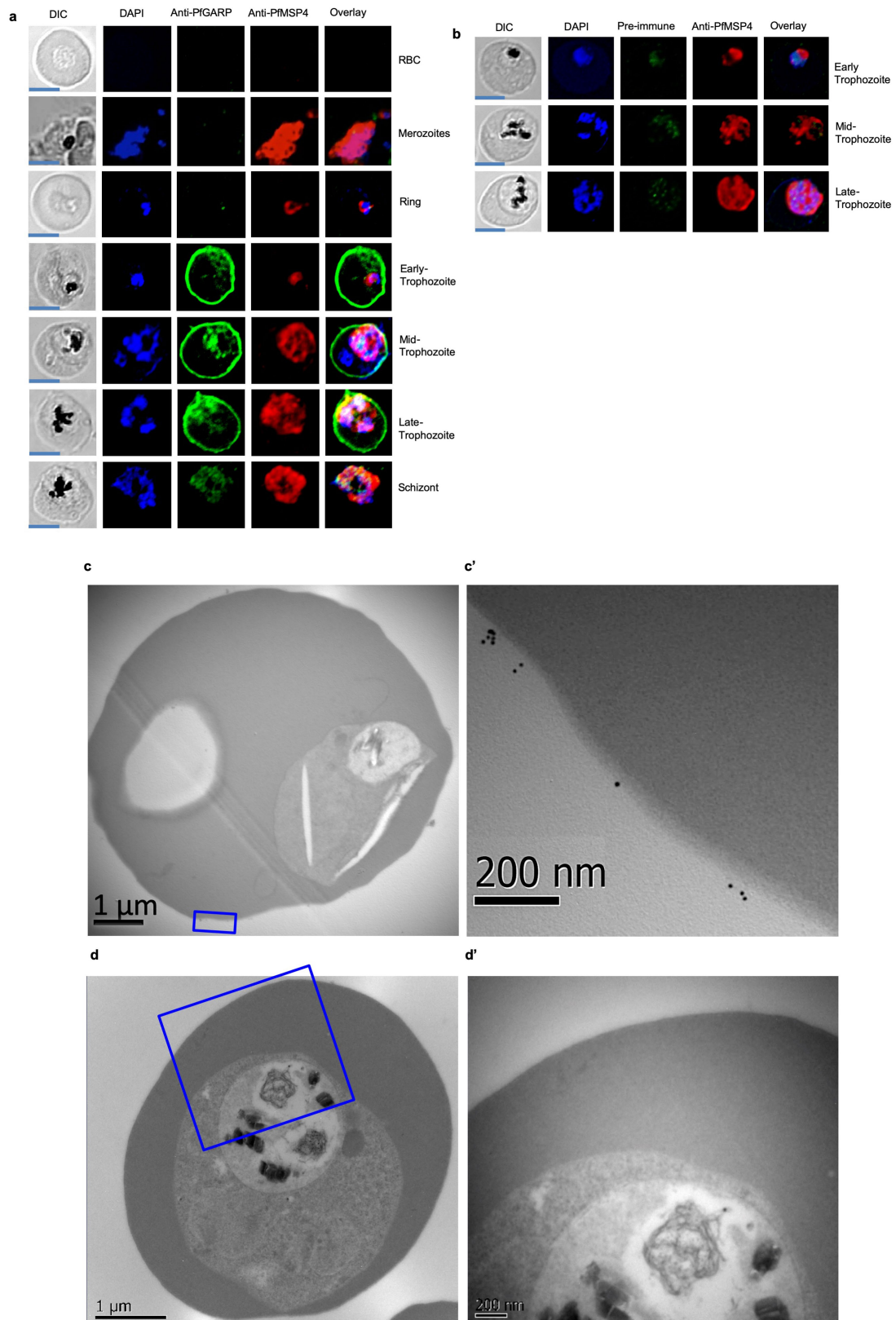
**Extended Data Fig. 3 | Construction and characterization of the 3D7-PfGARP KD parasite line.** **a**, Targeting strategy for creating 3D7-PfGARP KD parasites. **b**, Immunoblot analysis of 3D7-PfGARP KD parasites. Parasites were sorbitol-synchronized at the ring stage, incubated with or without anhydrotetracycline (ATc) for 20 h and blots were probed with anti-V5. The expected molecular weight of the PfGARP V5-tagged protein is 124 kDa; however, its apparent mobility is 165 kDa owing to its acidic composition. Lane 1, uninfected RBCs; lane 2, RBCs infected with 3D7-PfGARP KD parasites and cultured without anhydrotetracycline; lane 3, RBCs infected with 3D7-PfGARP KD parasites and cultured with anhydrotetracycline. **c**, **d**, Expression of PfGARP on the surface of human RBCs infected with 3D7-PfGARP KD parasites. Ring-stage 3D7-PfGARP KD parasites were cultured to the trophozoite stage in the absence (**c**) or presence (**d**) of anhydrotetracycline. Expression of PfGARP

on the surface of fixed but not permeabilized infected human RBCs was determined by flow cytometry, using monoclonal anti-V5 as the primary and anti-mouse IgG-Alexa Fluor 488 as the secondary antibody. Infected RBCs were gated and identified as described in Fig. 1e. **e**, Growth curves for 3D7-PfGARP KD parasites. Ring-stage parasites were cultured with or without anhydrotetracycline. Parasitaemia was measured by microscopy. Data are mean  $\pm$  s.e.m. of three biologically independent replicates. **f**, GIAs using 10% anti-rPfGARP-A serum or pre-immune serum on 3D7-PfGARP KD parasites cultured with or without anhydrotetracycline. Data are mean  $\pm$  s.e.m. of three biologically independent replicates. The *P* value was calculated by non-parametric two-sided Mann-Whitney *U*-test. Data are representative of three independent experiments (**b**, **d**, **e**, **f**) or five independent experiments (**c**).



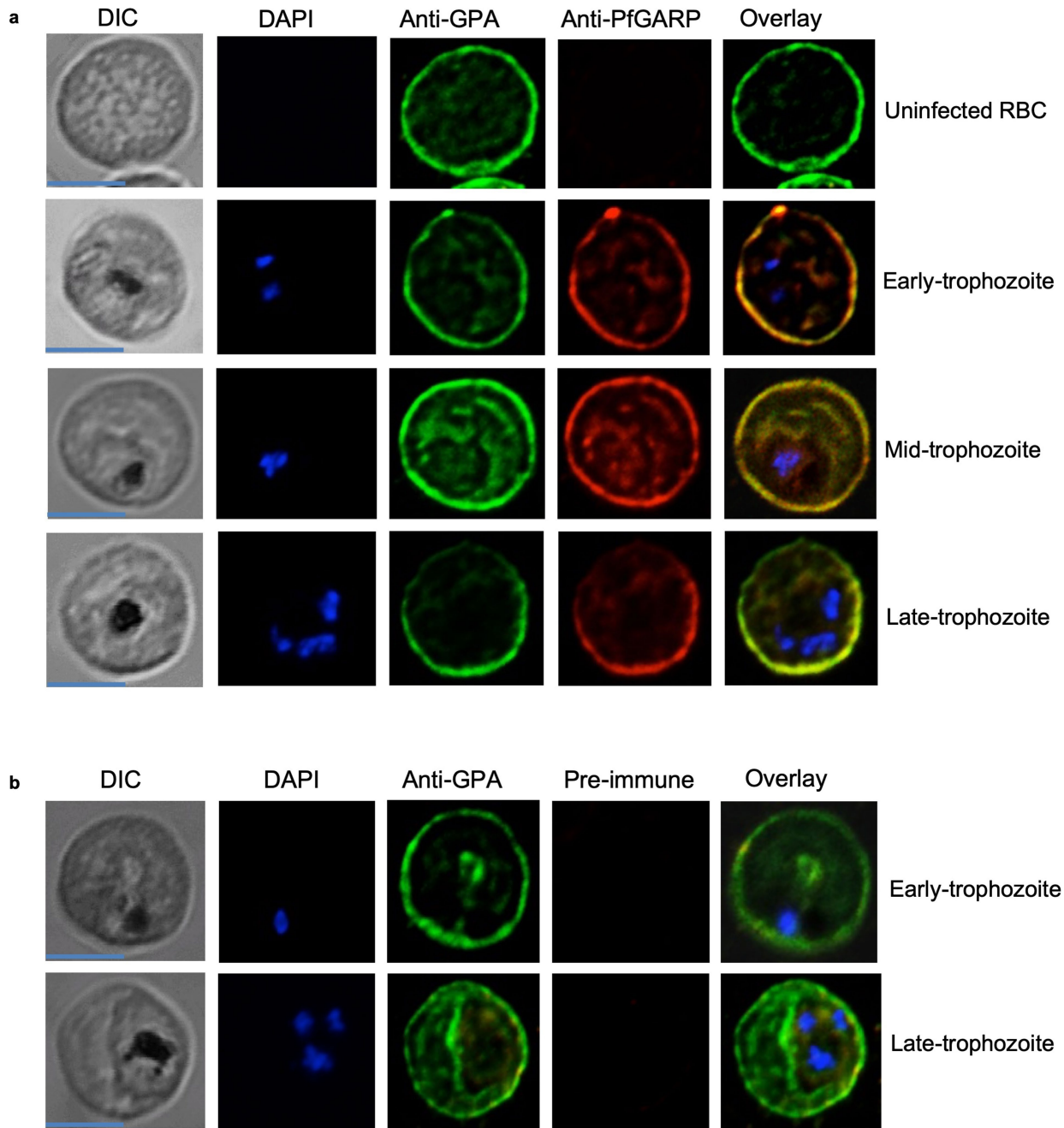
**Extended Data Fig. 4 | Construction and characterization of the 3D7-PfGARP KO parasite line.** **a**, Targeting strategy for creating 3D7-PfGARP KO parasites, **b**, Immunoblot analysis of 3D7-PfGARP KO. Trophozoite-stage 3D7 wild-type or 3D7-PfGARP KO parasites were probed with anti-PfGARP, and with anti-histone H3 as a loading control. Lane 1, RBCs infected with 3D7-PfGARP KO parasites; lane 2, RBCs infected with 3D7 wild-type parasites. **c**, **d**, Expression of PfGARP on the surface of human RBCs (fixed but not permeabilized) infected with 3D7-PfGARP KO parasites. Ring-stage stage 3D7 wild-type or 3D7-PfGARP KO parasites were cultured to the trophozoite stage. Expression of PfGARP was determined by flow cytometry, using anti-PfGARP as the primary and anti-mouse IgG-Alexa Fluor 488 as the secondary antibody. Infected RBCs were gated and identified as described in Fig. 1e. **e**, Growth

curves for 3D7-PfGARP KO parasites. Ring-stage 3D7 wild-type or 3D7-PfGARP KO parasites were plated at 0.5% parasitaemia and cultured for 6 days. Parasitaemia was measured by microscopy. Data are mean  $\pm$  s.e.m. of three biologically independent replicates. **f**, Ring-stage 3D7 wild-type or 3D7-PfGARP KO parasites with targeted deletion of *PfGARP* were cultured at a 1:10 dilution in the presence of anti-PfGARP-A mouse serum that was generated by immunizing mice with PfGARP-A-mRNA LNPs. Negative controls were no antiserum (blue) and pre-immune mouse serum (red). Parasites were cultured for 48 h at 37 °C and ring-stage and early-trophozoite-stage parasites were counted by microscopy. Data are mean  $\pm$  s.e.m. of six biologically independent replicates. *P* values were calculated by non-parametric two-tailed Mann-Whitney *U*-test. Data are representative of two independent experiments.



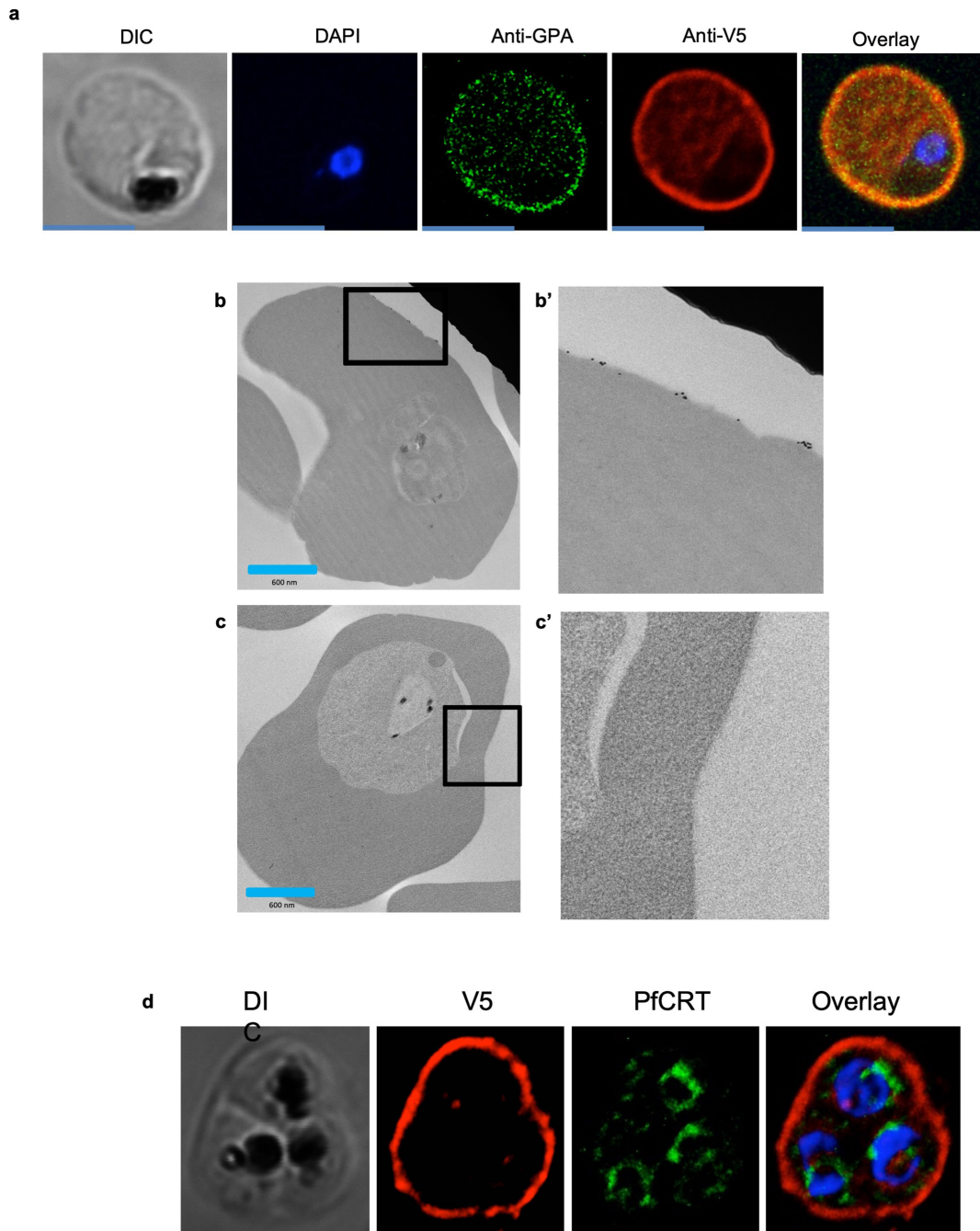
**Extended Data Fig. 5 | Immunolocalization of PfGARP.** **a**, Uninfected and infected RBCs were probed with mouse anti-PfGARP prepared by DNA vaccination (green) and with rabbit anti-PfMSP4 (red) and counterstained with DAPI to label parasite nuclei. PfGARP is detected on the membranes of RBCs infected with early-, mid- and late-trophozoite-stage parasites and does not colocalize with PfMSP4 (which localizes to the parasite membrane). DIC, differential interference contrast microscopy. Scale bars, 5  $\mu$ m. **b**, Trophozoite-infected RBCs do not label when probed with pre-immune

mouse serum. Scale bars, 5  $\mu$ m. **c, d**, Non-permeabilized, unfixed trophozoite-infected RBCs were incubated with polyclonal anti-rPfGARP (**c**) or control mouse serum (**d**), probed with anti-mouse IgG labelled with 10-nm gold particles, fixed, embedded and visualized by transmission electron microscopy. PfGARP localized to the outer leaflet of trophozoite-infected RBCs. Right, higher-magnification views of the boxed areas on the left. Images are representative of five (**a, b**) or two (**c, d**) biologically independent experiments.



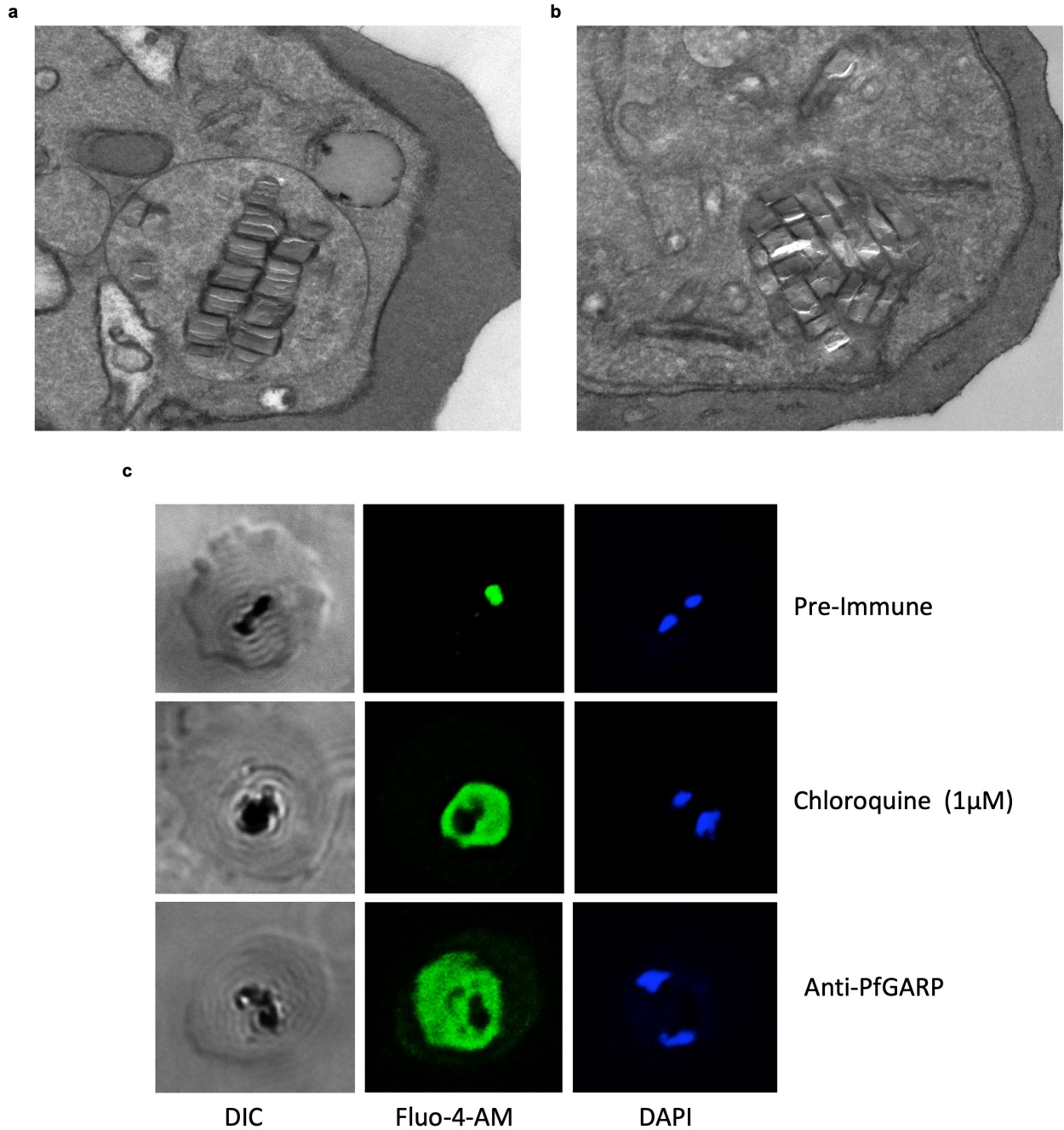
**Extended Data Fig. 6 | PfGARP colocalizes with glycophorin A to the exofacial surface of trophozoite-infected RBCs. a**, Uninfected and infected RBCs were probed with rabbit anti-glycophorin A (anti-GYPA; green) and mouse anti-PfGARP prepared by DNA vaccination (red) and counterstained with DAPI to label parasite nuclei. PfGARP is detected only in

trophozoite-infected RBCs and colocalizes with human glycophorin A on the RBC membrane. Scale bars, 5  $\mu$ m. **b**, Neither early- nor late-trophozoite-stage-infected RBCs label when probed with pre-immune mouse serum. Scale bars, 5  $\mu$ m. Images are representative of three independent experiments (**a**, **b**).



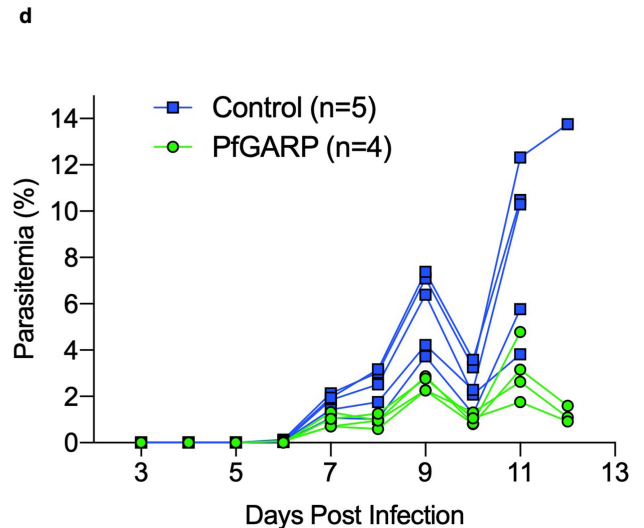
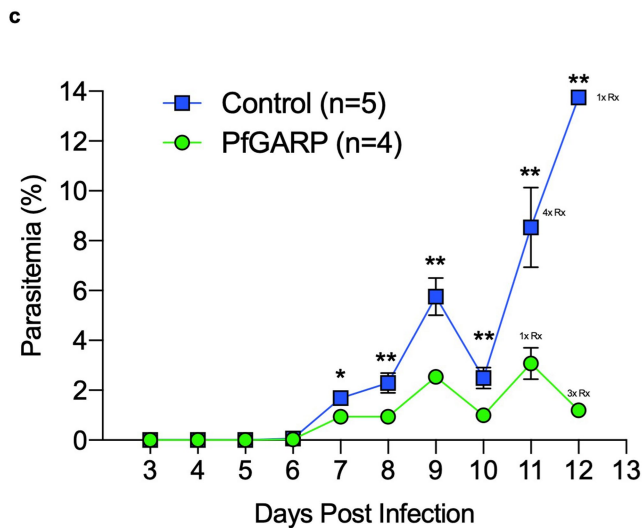
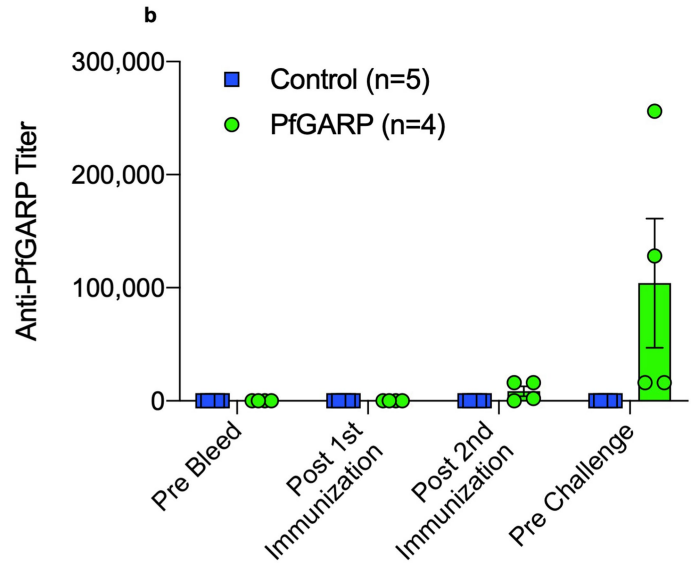
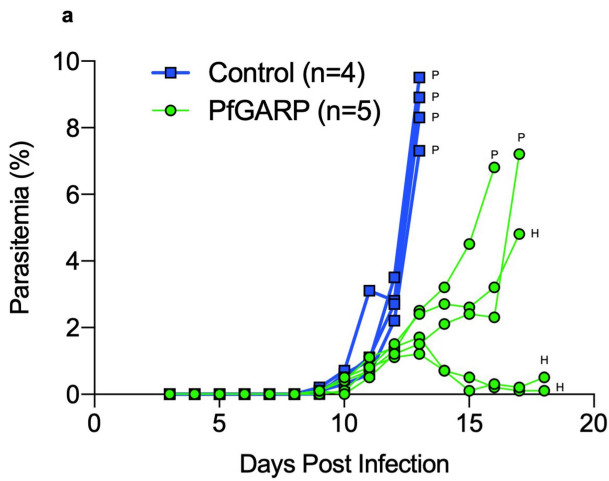
**Extended Data Fig. 7 | Localization of V5-tagged PfGARP.** **a**, 3D7-PfGARP KD parasites, in which PfGARP is tagged with the V5 epitope, were grown in the presence of anhydrotetracycline to induce the expression of PfGARP, probed with rabbit anti-glycophorin A (green) and mouse anti-V5 (red) antibodies and counterstained with DAPI to label parasite nuclei. V5-tagged PfGARP colocalizes with glycophorin A to the exofacial surface of trophozoite-infected, non-permeabilized RBCs. Scale bars, 5  $\mu$ m. **b**, 3D7-PfGARP KD parasites were grown in the presence of anhydrotetracycline to induce the expression of PfGARP. RBCs infected with trophozoite-stage 3D7-PfGARP KD parasites were fixed and incubated with anti-V5 mouse IgG (**b**) or buffer (**c**) and probed with

anti-mouse IgG labelled with 10-nm gold particles. V5-tagged PfGARP localized to the outer leaflet of 3D7-PfGARP KD-infected, non-permeabilized RBCs. Right, higher-magnification views of the boxed areas on the left. **d**, 3D7-PfGARP KD parasites were grown in the presence of anhydrotetracycline to induce the expression of PfGARP, probed with anti-PfCRT (green) and anti-V5 (red) antibodies and counterstained with DAPI to label parasite nuclei. PfGARP does not colocalize with PfCRT to the food vacuole in the majority of trophozoite-infected RBCs. Images are representative of three (**a**), two (**b**, **c**) or five (**d**) biologically independent experiments.



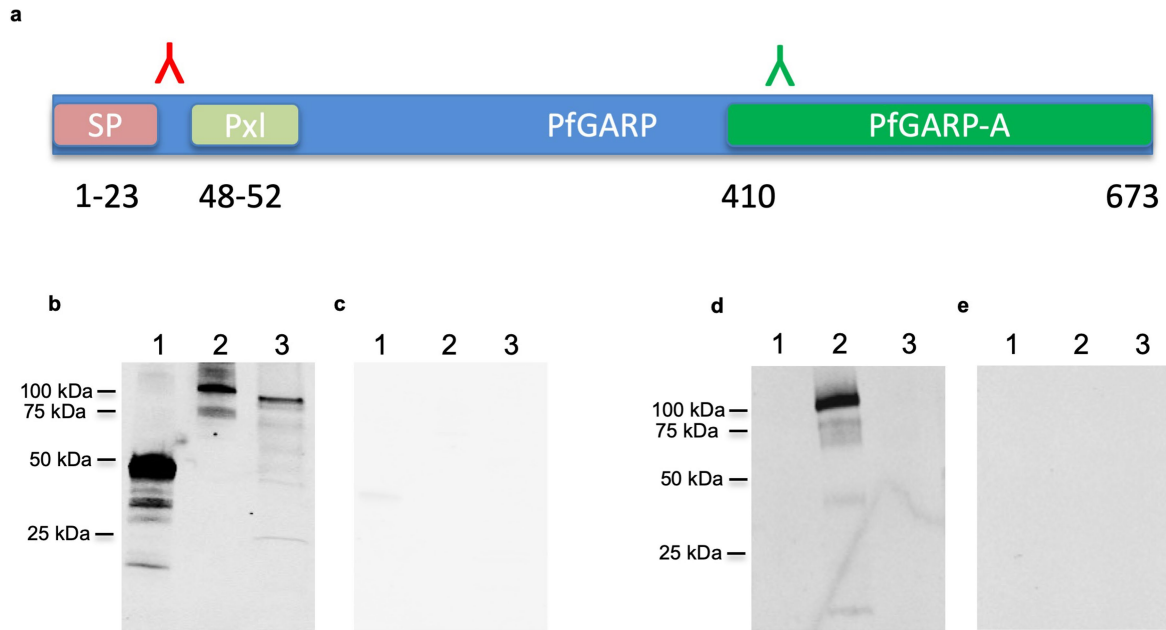
**Extended Data Fig. 8 | Anti-PfGARP antibodies disrupt the integrity of the food vacuole.** 3D7 parasites were synchronized to the ring stage and plated at 5% parasitaemia in the presence of pre-immune (a) or anti-rPfGARP-A (b) mouse serum at a 1:10 dilution. Parasites were cultured for 24 h and processed for transmission electron microscopy. Data are representative of all

trophozoites observed in three biologically independent experiments (a, b). c, Ring-stage 3D7 parasites were treated with pre-immune or anti-PfGARP serum (1:10) or 1 µM chloroquine for 24 h, followed by staining with DAPI and Fluo-4 AM. Data are representative of two biologically independent experiments.



**Extended Data Fig. 9 | Vaccination with PfGARP protects monkeys from *P. falciparum* challenge.** **a**, Individual parasitaemia data from the monkey trial presented in Fig. 4. *Aotus* monkeys vaccinated with PfGARP-A-mRNA LNPs ( $n=5$ ) and control monkeys vaccinated with poly(C)-RNA LNPs ( $n=4$ ) were challenged intravenously with  $1 \times 10^4$  *P. falciparum*-infected RBCs and parasitaemia was followed daily. H indicates treatment for low haemoglobin; P indicates treatment for high parasitaemia. **b**, Animals were injected subcutaneously either with 50  $\mu$ g of rPfGARP-A emulsified in 100  $\mu$ l Ribi ( $n=4$  monkeys) or with Ribi alone (negative control;  $n=5$  monkeys) at weeks 0, 3 and 6, and PfGARP-A-specific IgG titres were determined. Data are mean  $\pm$  s.e.m. **c**, Vaccinated *Aotus* monkeys were challenged intravenously with  $10^4$

*P. falciparum* FVO strain-infected RBCs on day 63 and parasitaemia was followed daily. Data are mean  $\pm$  s.e.m. Control monkeys had significantly higher parasitaemia on days 7–12 than monkeys immunized with PfGARP. On day 11, the final day with complete follow-up of all monkeys, control monkeys had 3.5-fold-higher parasitaemia than PfGARP-vaccinated monkeys. Four control monkeys met pre-specified criteria for drug treatment on day 11 and the remaining control monkey met these criteria on day 12. On day 11, one PfGARP-vaccinated monkey underwent drug treatment despite not meeting the pre-specified criteria. \* $P < 0.05$ , \*\* $P < 0.01$  in two-sided  $t$ -tests without adjustment for multiple comparisons. **d**, Parasitaemia data from the individual monkeys in **c**.



**Extended Data Fig. 10 | The PEXEL motifs processed and cleaved in mature PfGARP.** **a**, Schematic depicting the binding sites for the peptide-specific antibodies. **b–e**, Immunoblot of rPfGARP-A (lane 1), recombinant full-length PfGARP (lane 2) and an extract of trophozoite-infected RBCs (lane 3) probed with antibodies raised against amino acids 504–522 of PfGARP (**b**) or pre-immune serum (**c**), or with antibodies raised against amino acids 31–48 of

PfGARP (**d**) or pre-immune serum (**e**). Only antibodies raised against amino acids 504–522 recognized native PfGARP in trophozoite-infected RBCs, whereas antibodies raised against amino acids 31–48 only recognized the full-length recombinant PfGARP, confirming that the PEXEL motif is cleaved during the processing of native PfGARP. Pxl, PEXEL motif; SP, signal peptide. Data are representative of three biologically independent experiments.

## Reporting Summary

Nature Research wishes to improve the reproducibility of the work that we publish. This form provides structure for consistency and transparency in reporting. For further information on Nature Research policies, see [Authors & Referees](#) and the [Editorial Policy Checklist](#).

### Statistics

For all statistical analyses, confirm that the following items are present in the figure legend, table legend, main text, or Methods section.

n/a Confirmed

- The exact sample size ( $n$ ) for each experimental group/condition, given as a discrete number and unit of measurement
- A statement on whether measurements were taken from distinct samples or whether the same sample was measured repeatedly
- The statistical test(s) used AND whether they are one- or two-sided  
*Only common tests should be described solely by name; describe more complex techniques in the Methods section.*
- A description of all covariates tested
- A description of any assumptions or corrections, such as tests of normality and adjustment for multiple comparisons
- A full description of the statistical parameters including central tendency (e.g. means) or other basic estimates (e.g. regression coefficient) AND variation (e.g. standard deviation) or associated estimates of uncertainty (e.g. confidence intervals)
- For null hypothesis testing, the test statistic (e.g.  $F$ ,  $t$ ,  $r$ ) with confidence intervals, effect sizes, degrees of freedom and  $P$  value noted  
*Give  $P$  values as exact values whenever suitable.*
- For Bayesian analysis, information on the choice of priors and Markov chain Monte Carlo settings
- For hierarchical and complex designs, identification of the appropriate level for tests and full reporting of outcomes
- Estimates of effect sizes (e.g. Cohen's  $d$ , Pearson's  $r$ ), indicating how they were calculated

*Our web collection on [statistics for biologists](#) contains articles on many of the points above.*

### Software and code

Policy information about [availability of computer code](#)

Data collection

Filemaker Pro v10

Data analysis

SAS v9, JMP v14 and Amira v2019.2

For manuscripts utilizing custom algorithms or software that are central to the research but not yet described in published literature, software must be made available to editors/reviewers. We strongly encourage code deposition in a community repository (e.g. GitHub). See the Nature Research [guidelines for submitting code & software](#) for further information.

### Data

Policy information about [availability of data](#)

All manuscripts must include a [data availability statement](#). This statement should provide the following information, where applicable:

- Accession codes, unique identifiers, or web links for publicly available datasets
- A list of figures that have associated raw data
- A description of any restrictions on data availability

The datasets generated during and/or analysed during the current study are available from the corresponding author on reasonable request

## Field-specific reporting

Please select the one below that is the best fit for your research. If you are not sure, read the appropriate sections before making your selection.

- Life sciences       Behavioural & social sciences       Ecological, evolutionary & environmental sciences

For a reference copy of the document with all sections, see [nature.com/documents/nr-reporting-summary-flat.pdf](https://www.nature.com/documents/nr-reporting-summary-flat.pdf)

## Life sciences study design

All studies must disclose on these points even when the disclosure is negative.

Sample size	Both cohort studies were based on open enrolment of participants living in the malaria endemic villages under study.
Data exclusions	no data was excluded
Replication	two independent cohorts were assessed. For in vitro experiments, multiple independent replicates were performed and all were successful.
Randomization	no formal randomization was performed
Blinding	slide readers (enumeration of parasitemia) were blind to treatment status for human blood films, in vitro assays, and the monkey vaccine experiments.

## Reporting for specific materials, systems and methods

We require information from authors about some types of materials, experimental systems and methods used in many studies. Here, indicate whether each material, system or method listed is relevant to your study. If you are not sure if a list item applies to your research, read the appropriate section before selecting a response.

### Materials & experimental systems

n/a	Involvement in the study
<input type="checkbox"/>	<input checked="" type="checkbox"/> Antibodies
<input type="checkbox"/>	<input checked="" type="checkbox"/> Eukaryotic cell lines
<input checked="" type="checkbox"/>	<input type="checkbox"/> Palaeontology
<input type="checkbox"/>	<input checked="" type="checkbox"/> Animals and other organisms
<input type="checkbox"/>	<input checked="" type="checkbox"/> Human research participants
<input type="checkbox"/>	<input checked="" type="checkbox"/> Clinical data

### Methods

n/a	Involvement in the study
<input checked="" type="checkbox"/>	<input type="checkbox"/> ChIP-seq
<input type="checkbox"/>	<input checked="" type="checkbox"/> Flow cytometry
<input checked="" type="checkbox"/>	<input type="checkbox"/> MRI-based neuroimaging

## Antibodies

Antibodies used

Antibodies Catalog no. Clone Lot no. Company  
 F(ab')<sub>2</sub>-Goat anti-Rabbit IgG (H+L) Cross-Adsorbed Secondary Antibody, Alexa Fluor 488 A-11070 853487 Invitrogen Molecular Probes  
 Goat anti-Mouse IgG (H+L) Highly Cross-Adsorbed Secondary Antibody, Alexa Fluor 594 A-11032 1985396 Invitrogen Molecular Probes  
 Goat anti-Rat IgG (H+L) Cross-Adsorbed Secondary Antibody, Alexa Fluor 488 A-A11006 1423045 Invitrogen Molecular Probes  
 F(ab')<sub>2</sub>-Goat anti-Mouse IgG, IgM (H+L) Secondary Antibody, Alexa Fluor 488 A10684 891190 Invitrogen Molecular Probes  
 Goat anti-Rabbit IgG (H+L) Secondary Antibody, Alexa Fluor 488-5 nm colloidal gold A31565 764359 Invitrogen Molecular Probes  
 IRDye 800CW Goat anti-Rabbit IgG (H + L) Secondary Antibody 926-32211 C30829-02 ODYSSEY imaging system 926-68070 C30723-04 ODYSSEY imaging system  
 FITC anti-human CD235a (Glycophorin A) Antibody 349103 HI264 B138023 BioLegend Inc.  
 Biotin Mouse anti-human IgG 555784 5288794 BD Biosciences  
 APC anti-human CD235a (Glycophorin A), 349113 Clone-HI 264 B262669 Biolegend Inc.  
 V5-Tag Monoclonal antibody R960-25 1937181 Thermo Fisher Scientific

Validation

manufacturer validated each antibody for the intended application

## Eukaryotic cell lines

Policy information about [cell lines](#)

Cell line source(s)	NIH repository (MR4)
Authentication	none
Mycoplasma contamination	not tested

Commonly misidentified lines  
(See [ICLAC](#) register)

none used

## Animals and other organisms

Policy information about [studies involving animals](#); [ARRIVE guidelines](#) recommended for reporting animal research

Laboratory animals

Mice  
BALB/cJ both male and female mice (The Jackson Laboratory). Ages 20-26 weeks.

Monkey  
Aotus nancymaae Both male and female (MD Anderson Cancer Center). Adults, age unknown.

Wild animals

none

Field-collected samples

none

Ethics oversight

Animal studies approved by IACUC of Brown University, Rhode Island Hospital and the NIH

Note that full information on the approval of the study protocol must also be provided in the manuscript.

## Human research participants

Policy information about [studies involving human research participants](#)

Population characteristics

Tanzanian Birth cohort (age 0 to 4 years)  
Kenyan Cohort, males only, ages 12-35  
Further details can be found in the MS as well as ref #19 (Kenyan cohort) and ref #2 (Tanzanian cohort)

Recruitment

Kenyan cohort: Open recruitment in the designated malaria endemic villages. Details provided in ref#19  
Tanzanian Cohort: Open recruitment at delivery facilities. Details provided in Ref #2.

Ethics oversight

Ethical clearance was obtained from the IRBs of SBRI and Rhode Island Hospital, the Medical Research Coordinating Committee of the National Institute for Medical Research, Tanzania, and the Kenyan Medical Research Institute.

Note that full information on the approval of the study protocol must also be provided in the manuscript.

## Clinical data

Policy information about [clinical studies](#)

All manuscripts should comply with the ICMJE [guidelines for publication of clinical research](#) and a completed [CONSORT checklist](#) must be included with all submissions.

Clinical trial registration

This is not a clinical trial.

Study protocol

*Note where the full trial protocol can be accessed OR if not available, explain why.*

Data collection

*Describe the settings and locales of data collection, noting the time periods of recruitment and data collection.*

Outcomes

*Describe how you pre-defined primary and secondary outcome measures and how you assessed these measures.*

## Flow Cytometry

Plots

Confirm that:

- The axis labels state the marker and fluorochrome used (e.g. CD4-FITC).
- The axis scales are clearly visible. Include numbers along axes only for bottom left plot of group (a 'group' is an analysis of identical markers).
- All plots are contour plots with outliers or pseudocolor plots.
- A numerical value for number of cells or percentage (with statistics) is provided.

## Methodology

Sample preparation

After treatment in culture, the infected RBCs were harvested and washed two times with PBS. After thorough washing, RBCs were appropriately stained and suspended in PBS before acquisition and analysis by using flow cytometer.

Instrument

BD LSR II Flow Cytometer was used for data collection

Software	BD FACS Diva 6.1.1 was used for data collection Flowjo vX.0.7 was used for data analysis
Cell population abundance	No sorting was done in the study; Infected RBCs were identified and gated using standard markers
Gating strategy	Single cells were gated using SSC-H and SSC-A; Normal and Infected RBCs were identified and gated by using Hoechst 33342 and APC conjugated anti-human Glycophorin A antibody. Infected RBCs were identified as cells which were positive for both Glycophorin A and Hoechst 33342. Normal RBCs were identified as cells which were positive for Glycophorin A but negative for Hoechst 33342. Among the infected RBCs, the cells, which were positive for JC-1 red high, represent live parasites and cells, which were JC-1, red low, represent dead parasites. Gating strategy provided in the main Figure 3 H and I.

Tick this box to confirm that a figure exemplifying the gating strategy is provided in the Supplementary Information.